

Plasticity of Tyrosine Hydroxylase and Serotonergic Systems in the Regenerating Spinal Cord of Adult Zebrafish

Veronika Kuscha, Antón Barreiro-Iglesias, Catherina G. Becker, and Thomas Becker*

Centre for Neuroregeneration, School of Biomedical Sciences, University of Edinburgh, Edinburgh EH16 4SB, United Kingdom

ABSTRACT

Monoaminergic innervation of the spinal cord has important modulatory functions for locomotion. Here we performed a quantitative study to determine the plastic changes of tyrosine hydroxylase-positive ($TH1^+$; mainly dopaminergic), and serotonergic ($5-HT^+$) terminals and cells during successful spinal cord regeneration in adult zebrafish. $TH1^+$ innervation in the spinal cord is derived from the brain. After spinal cord transection, $TH1^+$ immunoreactivity is completely lost from the caudal spinal cord. Terminal varicosities increase in density rostral to the lesion site compared with unlesioned controls and are re-established in the caudal spinal cord at 6 weeks post lesion. Interestingly, axons mostly fail to re-innervate more caudal levels of the spinal cord even after prolonged survival times. However, densities of terminal

varicosities correlate with recovery of swimming behavior, which is completely lost again after re-lesion of the spinal cord. Similar observations were made for terminals derived from descending $5-HT^+$ axons from the brain. In addition, spinal $5-HT^+$ neurons were newly generated after a lesion and transiently increased in number up to fivefold, which depended in part on hedgehog signaling. Overall, $TH1^+$ and $5-HT^+$ innervation is massively altered in the successfully regenerated spinal cord of adult zebrafish. Despite these changes in TH and $5-HT$ systems, a remarkable recovery of swimming capability is achieved, suggesting significant plasticity of the adult spinal network during regeneration. J. Comp. Neurol. 520:933–951, 2012.

© 2011 Wiley Periodicals, Inc.

INDEXING TERMS: regeneration; $5-HT$; tyrosine hydroxylase; sonic hedgehog; neurogenesis

Adult zebrafish, in contrast to mammals, are capable of successful spinal cord regeneration, such that plastic changes in cellular and axonal compartments that are associated with functional regeneration can be studied in this genetically tractable vertebrate (Becker and Becker, 2007). We have previously shown that the number of supraspinal neurons that grow axons beyond a spinal lesion site correlates with recovery of swimming capability (Becker et al., 1997). Moreover, when regeneration over a spinal lesion site in goldfish (Bernstein and Bernstein, 1969) or zebrafish is mechanically blocked, no recovery occurs. The same is true when re-growth of descending axons is selectively compromised by knock down of L1.1, a cell recognition molecule necessary for axon re-growth (Becker et al., 2004). Thus axon re-growth beyond the lesion site is crucial for recovery from a spinal lesion. However, recovery is seen in eel (Doyle et al., 2001) and lamprey (McClellan, 1994) already when axons have only grown for a short distance into the distal cord, indicating that the spinal circuitry can produce swimming

patterns without complete re-innervation of the distal cord.

In addition, a lesion induces neurogenesis in the spinal cord of teleost fish (for a recent review, see Sirbulescu and Zupanc, 2010), including zebrafish (Reimer et al., 2008). Elucidating the changes that specific axon terminal and cellular systems undergo during regeneration on a quantitative basis may help to gauge the magnitude of overall plasticity that leads to the remarkable functional recovery in adult zebrafish after a spinal lesion.

Grant sponsor: the Biotechnological and Biological Science Research Council (BBSRC); Grant number: BB/H003304/1; Grant sponsors: the Robert Packard Center for Amyotrophic Lateral Sclerosis Research at Johns Hopkins; the Euan MacDonald Centre for Motor Neurone Disease Research; Crerar Hotels (generous contribution to the Euan MacDonald Centre toward the purchase of a confocal microscope).

The last two authors contributed equally to this work.

*CORRESPONDENCE TO: Thomas Becker, Centre for Neuroregeneration, School of Biomedical Sciences, University of Edinburgh, The Chancellor's Building, Edinburgh EH16 4SB, UK. E-mail: thomas.becker@ed.ac.uk.

Received May 7, 2011; Revised July 3, 2011; Accepted August 3, 2011

DOI 10.1002/cne.22739

Published online August 9, 2011 in Wiley Online Library (wileyonlinelibrary.com)

We decided to study changes in the dopaminergic and serotonergic systems, because both of these have been shown to critically influence the output of the spinal central pattern generator for locomotion (reviewed in Grillner and Jessell, 2009; Jordan et al., 2008). In larval zebrafish, dopaminergic innervation of the spinal cord is derived exclusively from the diencephalon (Kastenhuber et al., 2010; McLean and Fetcho, 2004). Dopamine suppresses initiation of swimming in pre-feeding larvae (Thirumalai and Cline, 2008), and the atypical antipsychotic clozapine, acting as an antagonist of the D4 receptor in zebrafish, causes hypoactivity in older embryos (Boehmler et al., 2007). In larval lampreys, dopamine inhibits glutamatergic reticulospinal transmission (Svensson et al., 2003) and increases or decreases fictive swimming frequency in a dose-dependent manner (McPherson and Kemnitz, 1994).

Serotonergic innervation of the spinal cord originates from supraspinal raphe neurons (Lillesaar et al., 2009) and from spinal intrinsic neurons (van Raamsdonk et al., 1996) in adult zebrafish. Endogenous serotonin decreases the frequency of *N*-methyl-D-aspartate (NMDA)-induced locomotor rhythms in fictive swimming of adult zebrafish spinal cord preparations by increasing mid-cycle inhibitory postsynaptic potentials and delaying the subsequent onset of hyperpolarization (Gabriel et al., 2009). Moreover, serotonin has been shown to directly modulate firing patterns of rat motor neurons (Kjaerulff and Kiehn, 2001).

Previous work has presented evidence for regeneration of dopaminergic and serotonergic axons in the spinal cord of zebrafish (van Raamsdonk et al., 1998). Also, in the spinal cord of the sea lamprey, regeneration of serotonergic descending axons has been reported (Cornide-Petronio et al., 2011). In addition, there is lesion-induced generation of serotonergic cells in the spinal cord of the closely related goldfish (Takeda et al., 2008). However, quantitative analyses of terminal densities necessary for a comparison of the potential functionality of the regenerated with the unlesioned situation are missing. We find that both dopaminergic and serotonergic systems undergo massive changes after a spinal lesion, with several anatomical parameters not returning to levels observed in unlesioned animals even after prolonged survival times. These changes include hyper-innervation of the rostral spinal cord, reduced re-innervation of the caudal spinal cord, and a lack of re-growth to more caudal levels for both systems. This suggests that considerable plasticity of the locomotor network occurs, leading to recovery of swimming function.

MATERIALS AND METHODS

Animals

All fish were kept and bred in our laboratory fish facility according to standard methods (Westerfield, 1989), and

all experimental procedures were approved by the British Home Office. We used wild-type (wik; ZFIN.org) and two transgenic lines.

To generate the *olig2* reporter line *tg(olig2:GFP)* (Shin et al., 2003), a large bacterial artificial chromosome containing the *olig2* promoter was used, increasing the likelihood of faithful reporter gene expression. We have previously shown by *in situ* hybridization for *olig2* that the transgene accurately reports *olig2*-expressing cells in the lesioned adult spinal cord (Reimer et al., 2009).

We also used *tg(shha:GFP)* (Shkumatava et al., 2004). This *sonic hedgehog* (*shh*) reporter line was generated by using 2.2 kb upstream of the start codon followed by sequences coding for *gfp* with a polyA signal. This was followed by a *NotI/KpnI* fragment of the *shh* locus (between +553 to +5,631) containing intron 1, exon 2, and intron 2. By using *in situ* hybridization for *shh*, we have previously shown that the transgene accurately reports *shh* expression in the adult lesioned spinal cord (Reimer et al., 2009). For simplicity, the lines are designated *olig2:GFP* and *shh:GFP* in this article.

Spinal lesion and intraperitoneal injections of substances

Lesions were performed as previously described (Becker et al., 1997). Fish were anesthetized in 0.033% aminobenzoic acid ethyl methyl ester (MS222; Sigma, St. Louis, MO). A longitudinal incision was made at the side of the fish to expose the vertebral column. The spinal cord was completely transected 3.5 mm caudal to the brainstem-spinal cord junction under visual control.

Bromodeoxyuridine (BrdU, B9285, Sigma) was injected intraperitoneally at a concentration of 5 mg/ml in a volume of 25 μ l phosphate-buffered saline (PBS; pH 7.4) at 0, 2, and 4 days post lesion (dpl), as described (Reimer et al., 2008). Analysis took place at 2 or at 6 weeks post lesion (wpl).

Cyclopamine (LC Laboratories, Woburn, MA) and the chemically related control substance tomatidine (Sigma) were injected at 10 mg/kg bodyweight at 3, 6, and 9 dpl, as previously described (Reimer et al., 2009). Analysis took place at 42 dpl.

Immunohistochemistry Antibody characterization

See Table 1 for the antibodies used. The anti-BrdU antisera labeled cell nuclei in the lesioned spinal cord only after prior incubation with BrdU. Thus, it does not cross-react nonspecifically with other antigens in the tissue of interest.

The anti-GFP serum specifically labels cellular structures only in green fluorescent protein (GFP) transgenic

TABLE 1.
Antibodies Used in This Study

Antigen	Immunogen	Manufacturer, species antibody was raised in, clone/cat. no.	Dilution
Bromodeoxyuridine (BrdU)	BrdU	Serotec (Munich, Germany), rat monoclonal, clone BU1/75 (ICR1)OBT0030CX	1:500
Green fluorescent protein (GFP)	Recombinant full-length protein	Abcam (Cambridge, UK), chicken polyclonal, ab13970	1:500
Tyrosine hydroxylase (TH)	Tyrosine hydroxylase purified from PC12 cells	Millipore (Temecula, CA), mouse monoclonal, clone LNC1MAB318	1:1,000
Dopamine	Dopamine-glutaraldehyde-bovine serum albumin (BSA) conjugate	H.W.M. Steinbusch (University of Maastricht, The Netherlands), rabbit polyclonal	1:750
Serotonin (5-HT)	Serotonin-creatinine sulfate-complex conjugated with formaldehyde to BSA	Sigma (St. Louis, MO), rabbit polyclonal, S5545	1:5000
Synaptic vesicle protein transmembrane glycoprotein (SV2)	Highly purified vesicles from the electric organ of <i>Discopyge ommata</i>	Developmental Studies Hybridoma Bank, (University of Iowa, Iowa City, IA), mouse monoclonal, SV2	1:20
Synaptophysin (syp)	Synthetic peptide corresponding to amino acids 270–291 of human syp (Herde et al., 2010)	Santa Cruz Biotechnology (Santa Cruz, CA), goat polyclonal, SYP(c-20): sc 7568	1:50

animals. Moreover, the labeling patterns are highly differential, e.g., in shh:GFP transgenic animals, only ventral ependymo-radial glial cells are labeled, and no ectopic labeling is detectable, demonstrating specific detection of the transgene.

Immunolabeling of the tyrosine hydroxylase 1 (TH1) antibody in embryos is abolished after antisense morpholino-mediated knockdown of *th1* in the embryonic zebrafish central nervous system (CNS; data not shown), strongly supporting specific labeling of TH1 by the antibody. The TH1 antibody has been shown to label exclusively TH1 protein in the zebrafish CNS (Chen et al., 2009). Chen et al. (2009) combined *in situ* hybridization for *th1* or *th2*, respectively, with immunohistochemical labeling by using the anti-TH1 antibody and found co-localization with *th1*, but not *th2* mRNA expression sites.

Labeling of the dopamine antiserum used was abolished in the brain of the teleost *Clarias gariepinus* by preincubation with dopamine, but not other monoamines (Corio et al., 1991). Recently, the serum was used to label dopaminergic axons in the brain of adult zebrafish (Yamamoto et al., 2011). Our labeling of circuitous fibers with numerous protrusions in the spinal cord was comparable to the labeling patterns of terminals found by Yamamoto et al. (2011). Importantly, we show a high degree of co-localization of dopamine with TH1 in double immunohistochemistry, which is to be expected, given that tyrosine hydroxylase is the rate-limiting enzyme for dopamine synthesis.

Preincubation of the anti-serotonin (5-HT) serum with 10^{-4} mol/L 5-HT abolished labeling in zebrafish tissue, thereby indicating specificity of the antiserum (Olsson et al., 2008).

The SV2 antiserum recognizes a highly conserved epitope in groups ranging from elasmobranchs to mammals

and shows glycosylated bands in Western blots between 75 and 85 kDa (Buckley and Kelly, 1985). The antibody is widely used in zebrafish (for example, Jing et al., 2009; Jonz and Nurse, 2003; Neill et al., 2004) and labels, for example, presynaptic terminals of motor axons, as determined by labeling of the postsynapse with bungarotoxin. When synapse formation is compromised in mutant zebrafish, SV2 labeling is absent (Boon et al., 2009), supporting specific labeling of the antibody. In agreement with our own observations, labeling was particularly intense in ventral and dorsal horns of the spinal cord of rats using this antibody (Buckley and Kelly, 1985).

The synaptophysin antiserum recognizes a single band of approximately 40 kDa in Western blots of mouse brain, rat brain, and PC12 cells according to the manufacturer's datasheet. In adult zebrafish, the antibody labels in a punctate pattern only in synaptic areas, which is very similar to that of SV2, supporting specific labeling.

Immunohistochemical procedures

Immunohistochemistry on 50-μm vibrating blade microtome sections has been described (Reimer et al., 2009), and followed the following protocol for most antibodies. Deeply anesthetized (0.1% MS222 for more than 5 minutes) fish were transcardially perfused with 4% paraformaldehyde (PFA) in PBS and postfixed in PFA overnight. If not stated otherwise, washing steps were 5 minutes at room temperature (RT). After transcardial perfusion, spinal cords or brains were embedded in agar (4% in PBS) and cut into 50-μm-thick sections on the Vibratome, and sections were collected in 24-well plates in PBS. For labeling of synaptophysin, antigen retrieval was performed by incubation at 80°C in citrate buffer (10 mM sodium citrate in PBS, pH 6.0) for 30 minutes. After

washing in PBS/0.1% Triton-X 100 (PBStx-0.1), sections were incubated in 50 mM glycine in PBStx-0.1 for 10 minutes followed by another 15-minute wash step in PBStx-0.1. For blocking, sections were incubated in either 1.5% donkey γ -globulin (synaptophysin labeling only) or normal goat serum for 30 minutes.

Incubation with one or two different primary antibodies in PBStx-0.1 was performed overnight or for 40 hours (synaptophysin labeling only) at 4°C. Subsequently sections were incubated with secondary antibodies (diluted 1:200; secondary Cy2-, Cy3-, and Cy5-conjugated antibodies were purchased from Jackson ImmunoResearch, West Grove, PA). Finally, the sections were mounted in 90% glycerol/PBS. Specific binding of the secondary antibody was controlled for by leaving out the primary antibody in alternating sections.

To detect BrdU, sections were washed in PBS/0.5% Triton-X-100 (PBStx-0.5) for 1 hour at RT, 3X in PBS, and 1X with HCl 37% diluted 1:8 in H₂O. Then sections were incubated in the diluted HCl at 37°C in the waterbath for 20 minutes. After washing 6X in PBS, sections were incubated in 50 mM glycine in PBS/0.3% Triton X-100 (PBStx-0.3) for 10 minutes followed by another 15-minute wash in PBStx-0.3. From here on, blocking and antibody incubations were performed as described above, except for the use of PBStx-0.3 instead of PBStx-0.1.

For simultaneous detection of dopamine and TH1, primary and secondary antibodies were simultaneously applied, and a modified protocol was used for primary antibody incubation: floating sections of spinal cords (50 μ m in thickness) of perfusion-fixed animals (2% PFA/2.5% glutaraldehyde, 1% metabisulfite) were washed in PBS/1% metabisulfite (pH adjusted to 7.4) with 0.1% Triton X-100 (PBS Mb Tx) for 15 minutes twice. Then sections were incubated in 0.1% NaBH₄ in twice distilled water for 30 minutes followed by two washing steps of 15 minutes each with PBS Mb Tx. Sections were blocked in 1.5% normal goat serum in PBS Mb Tx for 30 minutes. Then primary antibodies were diluted in PBS Mb Tx and incubated with the sections overnight at 4°C. Secondary antibody incubation followed the standard protocol. For documentation and analysis, we used either a Zeiss LSM 510 or a Zeiss 750 LSM confocal microscope with 20 \times and 63 \times oil lenses.

In situ hybridization

The method for nonradioactive in situ hybridization on 50- μ m vibrating blade microtome sections (Lieberoth et al., 2003) and the plasmids to generate probes for *th2* (Filippi et al., 2010) have been described. Solutions were made up with RNase-free water. If not stated otherwise, washing steps were 5 minutes long.

Sections of PFA-fixed tissue were transferred into 24-well-plates, washed twice in PBS/0.1% Tween-20

(PBST-0.1), and then digested with proteinase K (stock concentration: Roche [Mannheim, Germany] PCR Grade, 0.3 μ g/ml in 0.1 M Tris, pH 8, and 0.05 M EDTA; working solution: 0.7 μ l/ml) for 9 minutes at room temperature. After washing twice with glycine in PBST-0.1 (2 mg/ml), tissue was refixed in 4% PFA for 20 minutes. After washing 4X in PBST-0.1, supernatant was removed and sections were washed once in 300 μ l hybridization buffer (5 ml formamide, 2.5 ml 20X SSC, 10 μ l Tween, 100 μ l yeast tRNA [100 mg/ml], 2.38 ml DEPC-H₂O, 10 μ l heparin [50 mg/ml]). After replacing this with fresh hybridization buffer (500 μ l/well), the plate was wrapped with parafilm and kept at 55°C for at least 3 hours. Digoxigenin (DIG)-labeled probes (1:1,000 to 1:500 in hybridization buffer) were incubated at 80°C for 10 minutes, briefly centrifuged, and chilled on ice for 2 minutes. Hybridization buffer in the wells was replaced by probe solution. Plates were wrapped with parafilm and incubated at 55°C overnight. The following incubations were at 55°C. The solutions were preheated. Sections were washed twice in 50% formamide/2X SSC + 0.1% Tween-20 for 30 minutes each, once in 1X SSC + 0.1% Tween-20 for 15 minutes, and twice in 0.2X SSC + 0.1% Tween-20 for 30 minutes each.

Then the sections were blocked in 10% Boehringer/Roche blocking reagent (10 g blocking reagent in 100 ml PBST-0.1) at RT. Anti-DIG alkaline phosphatase-coupled fab fragments (Boehringer/Roche) were diluted 1:2,000 in blocking reagent, added to the sections, and left overnight at 4°C. Sections were washed 6 times for 20 minutes each in PBST-0.1 on a shaker and then once in PBS. Staining solution was prepared by adding one NBT/BCIP tablet (Sigma) in 10 ml twice distilled water. After washing once in staining solution, sections were incubated in fresh staining solution for 30 minutes to overnight, depending on the kinetics of signal development. Finally, sections were washed several times in PBS and mounted in 70% glycerol.

Retrograde axonal tracing combined with immunohistochemistry

Retrograde tracing of brain neurons with rhodamine dextran amine (RDA) or biocytin has been described (Becker et al., 1997). Briefly, a piece of recrystallized RDA or biocytin was applied to the completely transected spinal cord and allowed to be transported overnight (biocytin, detected with Cy-2-labeled streptavidin) or 6 days (RDA). Animals were perfusion-fixed, and brains were dissected and sectioned on a vibrating blade microtome and processed for immunohistochemistry as described above. The RDA and antibody signals were then detected by fluorescence microscopy.

Test of swimming capability

As previously described, we tested the swimming capability of lesioned fish by determining the time they were able to hold their position in a water current (Reimer et al., 2009). In a tunnel with a flat bottom (7-cm width), 15-cm-long compartments were divided off by wire mesh. A current of 7 cm/s was induced by using a pond pump (Nautilus 8000, Oase, Hörlstel, Germany). The time that fish were able to hold their position in the water current was recorded. When a fish was swept against the wire mesh and was unable to leave it again within 30 seconds, the experiment was stopped. Recovery was assumed after 1 hour of sustained swimming.

Axon and cell quantification

Counts of terminal varicosities

We observed TH1 and 5-HT immunoreactivity mainly in varicosities (Fig. 1G, 5B), which is typical of serotonergic and dopaminergic terminals (Leger et al., 2001; Mrini et al., 1995; Takeoka et al., 2009). Our manual and semiautomatic quantification method counts mostly profiles of varicosities. Occasionally, a fiber was too thick or too densely populated by varicosities to resolve these. Together with rare fibers of passage, these were then counted as single entities. Because the size and appearance of varicosities and axons was comparable between lesioned and unlesioned spinal cords, these quantifications give a good representation of changes in TH1⁺ and 5-HT⁺ innervation, which may be most relevant for a correlation with recovery of function. This method does not determine how many of the originally lesioned axons contribute to re-innervation of the spinal cord or increased density of varicosities in the rostral spinal cord.

We used a Zeiss LSM 510 confocal microscope with a 20× Apochromate 0.75 lens for acquiring images of whole spinal cross sections. To decrease background and increase edge and shape detection of the thin circuitous axonal structures, including varicosities, we used the Feature J Hessian plug-in for Image J (smallest eigenvalue Hessian tensor; smoothing scale to 1.0; <http://rsbweb.nih.gov/ij/plugins/index.html>) on maximum projection z-stacks (15 optical sections, thickness 1.5 μm) of whole spinal sections (50 μm in thickness) according to an established protocol (Grider et al., 2006). Upon conversion to binary images (threshold 140), mostly varicosities remain as particles and are quantified by using the “analyse particle” function of Image J with particle size 1 to infinity and circularity from 0.00 to 1.00. Comparing this method with manual counts showed a good correspondence. Images that contained fewer than approximately 100 varicosities were manually counted.

Cell quantification

Numbers of serotonergic cells were determined from stereological counts of confocal images of the three randomly selected 50-μm-thick Vibratome sections from the region up to 750 μm rostral to the lesion site and three sections 750 μm caudal to the lesion site. Numbers were calculated separately rostral and caudal to the lesion site and then summed for cell numbers in the entire 1.5 mm surrounding the lesion site.

Statistical analysis

For statistical analysis, the program Prism (GraphPad Software, La Jolla, CA) was used. Variability of values is given as SEM. Statistical significance was determined by using the Mann-Whitney U test for single comparisons or ANOVA followed by Dunnet's or Tukey's post test for multiple comparisons. Of note, numbers of cells and varicosity profiles in unlesioned animals did not show systematic changes over the period regeneration was analyzed in lesioned animals (up to 13 weeks of animals that were 5–10 month of age). Therefore, unlesioned controls were pooled.

Brightness and contrast of photomicrographs were adjusted and figure plates prepared by using Adobe Photoshop CS3 (Adobe Systems, San Jose, CA).

RESULTS

The aim of this study was to quantify the plastic changes in dopaminergic and serotonergic systems during successful spinal cord regeneration in an adult vertebrate.

Spinal dopamine is derived from the brain

To localize dopamine signals in the adult spinal cord, we analyzed the expression of TH1 and TH2, the rate-limiting enzymes for dopamine synthesis. Immunohistochemistry with a TH1-specific antibody (Chen et al., 2009) at a midthoracic level (~3.5 mm caudal to the brainstem/spinal cord transition) and at the level of the dorsal fin (~7 mm caudal to the brainstem/spinal cord transition) in unlesioned fish revealed circuitous axons with numerous varicosities, many of which were double-labeled with the synaptic marker synaptophysin (Fig. 1A–F,G–I). No TH1⁺ cell bodies were found in the spinal cord (Fig. 1A–C). Double immunohistochemistry with the dopamine antibody revealed that more than 80% of the TH1⁺ varicosities were dopaminergic, indicating that TH1⁺ terminals in the spinal cord are mainly dopaminergic (Fig. 1A–F,M). The remaining TH1⁺ profiles could be noradrenergic terminals, possibly originating from the locus coeruleus, as previously described at early developmental stages (Kastenhuber et al., 2010; McLean and Fetcho, 2004). In the regenerated spinal cord, caudal to the lesion site, a similar ratio of dopamine-positive TH1⁺ varicosities was observed, indicating that TH1 was a good

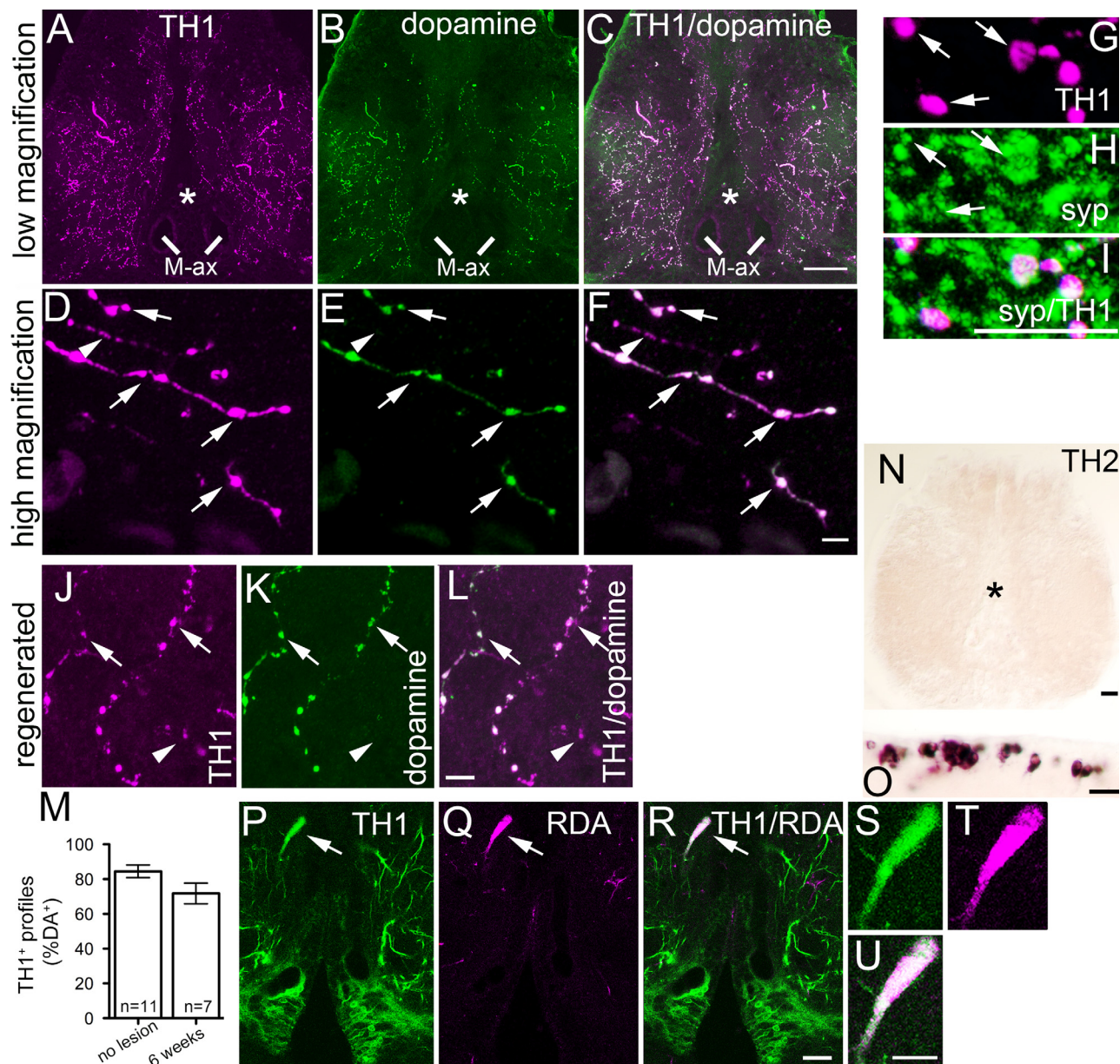


Figure 1. TH1⁺ axon terminals in the spinal cord are mostly dopaminergic and TH1⁺ and TH2⁺ cells are located only in the brain. A–F: Double labeling of TH1 and dopamine in spinal cross sections at a mid-thoracic level reveals overlap (arrows in D–F). An axon terminal labeled only by the TH1 antibody (arrowhead in D–F), the central canal (asterisk in A–C), and the Mauthner axons (M-ax in A–C) are indicated. G–I: TH1⁺ varicosities are co-labeled with synaptophysin (syp; arrows) immunoreactivity. J–L: Most regenerated TH1⁺ axon terminals in the spinal cord are dopaminergic at 6 weeks post lesion (arrows; a terminal that is only labeled by the TH1 antibody is indicated by an arrowhead). M: Quantification of TH1⁺ varicosity profiles double-labeled with a dopamine antibody (DA⁺) in the unlesioned situation and at 6 weeks post lesion indicates comparable ratios of TH1⁺ varicosities that are also dopamine positive. N,O: No mRNA expression for TH2 is detectable in spinal cross sections (N; asterisk indicates position of the central canal), but in a horizontal brain section in the posterior periventricular preoptic nucleus (O). P–R: In a cross section of the brain, a cell (arrow) in the periventricular nucleus of the posterior tuberculum is double-labeled by TH1 immunohistochemistry and retrograde tracing with RDA from a mid-thoracic level of the spinal cord. S–U: High magnification of the double-labeled cell in P–R. Scale bar = 40 μ m in C (applies to A–C); 5 μ m in F (applies to D–F), I (applies to G–I), and L (applies to J–L); 20 μ m in N and R (applies to P–R); 15 μ m in O; 10 μ m in U (applies to S–U). [Color figure can be viewed in the online issue, which is available at wileyonlinelibrary.com.]

marker for dopaminergic terminals also in the regenerated spinal cord (Fig. 1J–L,M).

To detect *th2*-expressing cell bodies in the CNS, we had to resort to *in situ* hybridization, because antibodies

reacting with TH2 were not available. This indicated the absence of TH2-expressing cells in the spinal cord (Fig. 1N). However, labeled cell bodies were found in a brain nucleus with spinal projections, the posterior

periventricular preoptic nucleus (Fig. 1O) (Becker et al., 1997). In agreement with a minor contribution of TH2⁺ axons to the dopaminergic innervation of the spinal cord, $10.4 \pm 3.19\%$ ($n = 2$ animals) of spinal terminal varicosities that were labeled by a dopamine antibody were TH1⁻.

To localize the source of TH1⁺ axons in the brain, we retrogradely traced the descending projection from a midthoracic level in combination with TH1 immunohistochemistry (Fig. 1P–U). This showed double-labeled cells in the dopaminergic periventricular nucleus of the posterior tuberculum in the diencephalon only, similar to what has been reported for the embryonic spinal cord (Kastenhuber et al., 2010; McLean and Fetcho, 2004). Overall, this suggests that the major sources of dopamine in the spinal cord are TH1⁺ axons coming from the brain and that TH1⁺ terminals are mostly dopaminergic. No spinal intrinsic cellular source of dopamine was detectable.

Lesion-induced quantitative changes in TH1⁺ terminal varicosities in the spinal cord

We examined the time course of changes in numbers of TH1⁺ varicosity profiles “rostral” (within 750 μm), “caudal” (within 750 μm), and “far caudal” (3,500 μm) to the position of a midthoracic lesion site (Fig. 2A) at 1, 2, 6, and 13 wpl. We chose these time points because severed axons in the caudal spinal cord have undergone Wallerian degeneration at 1 wpl, axon re-growth beyond the lesion site starts at around 2 wpl, and functional recovery plateaus at 6 wpl (Becker et al., 2004). We chose the 13 wpl time point to detect any late changes in innervation. For the late time points (6 and 13 wpl), when recovery can be assessed, values are only given for animals that showed recovery in a forced swim test, if not stated otherwise.

Rostral to the lesion site, from 2 weeks onward, numbers of TH1⁺ varicosity profiles continuously and significantly increased to at least 13 wpl (2 wpl: 952.6 ± 85.82 profiles/section, $n = 6$; 6 wpl: $1,204.6 \pm 145.36$, $n = 6$; 13 wpl: $1,571.9 \pm 368.55$, $n = 5$), the last time point examined, to levels that were 2.3-fold increased over those in unlesioned fish. This time course is consistent with initial die-back and later sprouting of axons (Fig. 2B–E).

Caudal to the lesion site, almost no varicosities were observed at 1 wpl (0.9 ± 0.61 profiles/section, $n = 5$), consistent with a supraspinal origin of these terminals and their subsequent Wallerian degeneration (Fig. 2F). Some varicosity profiles were visible at 2 wpl (24.8 ± 10.32 profiles/section, $n = 6$). At 6 wpl, a significant increase in the number of varicosity profiles (296.3 ± 80.57 profiles/section, $n = 6$; $P < 0.01$; Fig. 2G,I) was observed, compared with 1 wpl. This indicated re-growth and termination of TH1⁺ axons beyond the lesion site. At 13 wpl, 149.3 ± 124.35 profiles/section ($n = 4$; Fig. 2H,I) were observed.

Thus, immediately caudal to the lesion site, the number of TH1⁺ varicosity profiles was restored to maximally 44% of that in unlesioned animals at 6 wpl.

Far caudal to the midthoracic position of the lesion site, unlesioned animals showed substantial TH1⁺ innervation (484.6 ± 86.01 profiles/section, $n = 4$). This had disappeared by 1 wpl (1.7 ± 1.65 profiles/section, $n = 5$; Fig. 2J,M). Surprisingly, no appreciable re-innervation at this position was observed for up to 13 wpl (2 wpl: 2.8 ± 2.45 profiles/section, $n = 3$; 6 wpl: 3.3 ± 3.33 , $n = 6$; 13 wpl: 6.5 ± 2.77 , $n = 4$; Fig. 2K,L,M). This indicated that regenerating TH1⁺ axons did not reach previously innervated far caudal levels.

TH1⁺ re-innervation correlates with recovery of swimming capability

As previously reported, regenerative success in spinal-lesioned fish is variable, and anatomical regeneration of axons beyond the lesion site correlates with regenerative success (Becker et al., 1997, 2004). We wanted to determine whether plastic changes of TH1⁺ axon terminals also correlate with recovery of function. To assess recovery of swimming capability, we used a previously established test of forced swimming against a water flow at 6 wpl (Fig. 3A) (Reimer et al., 2009). In a set of 37 fish, we found that 17 fish were unable to hold their position in the water flow for more than 30 seconds. These fish were classified as nonrecovered. Another 17 fish held their position for an hour, at which time the test was terminated. These fish were classified as recovered. Unlesioned fish always sustained swimming to 1 hour. Three individuals that showed intermediate swim times (9, 13, and 50 minutes) were also classified as recovered (Fig. 3B). A comparison of numbers of TH1⁺ varicosity profiles rostral to the lesion site between recovered and nonrecovered fish did not show differences at 6 wpl (recovered: $1,204.6 \pm 145.36$ profiles/section, $n = 6$; nonrecovered: $1,011.4 \pm 115.82$, $n = 6$, $P > 0.05$; Fig. 4A–C).

In contrast, nonrecovered fish showed significantly less re-innervation caudal to the lesion site compared with recovered fish (recovered: 296.3 ± 80.57 profiles/section, $n = 6$; nonrecovered: 39.7 ± 32.31 , $n = 6$; $P < 0.05$; Fig. 4D–F). Thus quantitative differences in terminal varicosities caudal to the lesion site, derived from TH1⁺ axons that had grown beyond the lesion site, were correlated with recovery of swimming capability.

Re-lesion abolishes functional recovery and TH1⁺ axon terminals caudal to the lesion site

To determine whether recovery of swimming capability and TH1⁺ innervation of the caudal spinal cord depend on continuity of the spinal cord, we re-lesioned the spinal cord in the same position in three recovered animals that

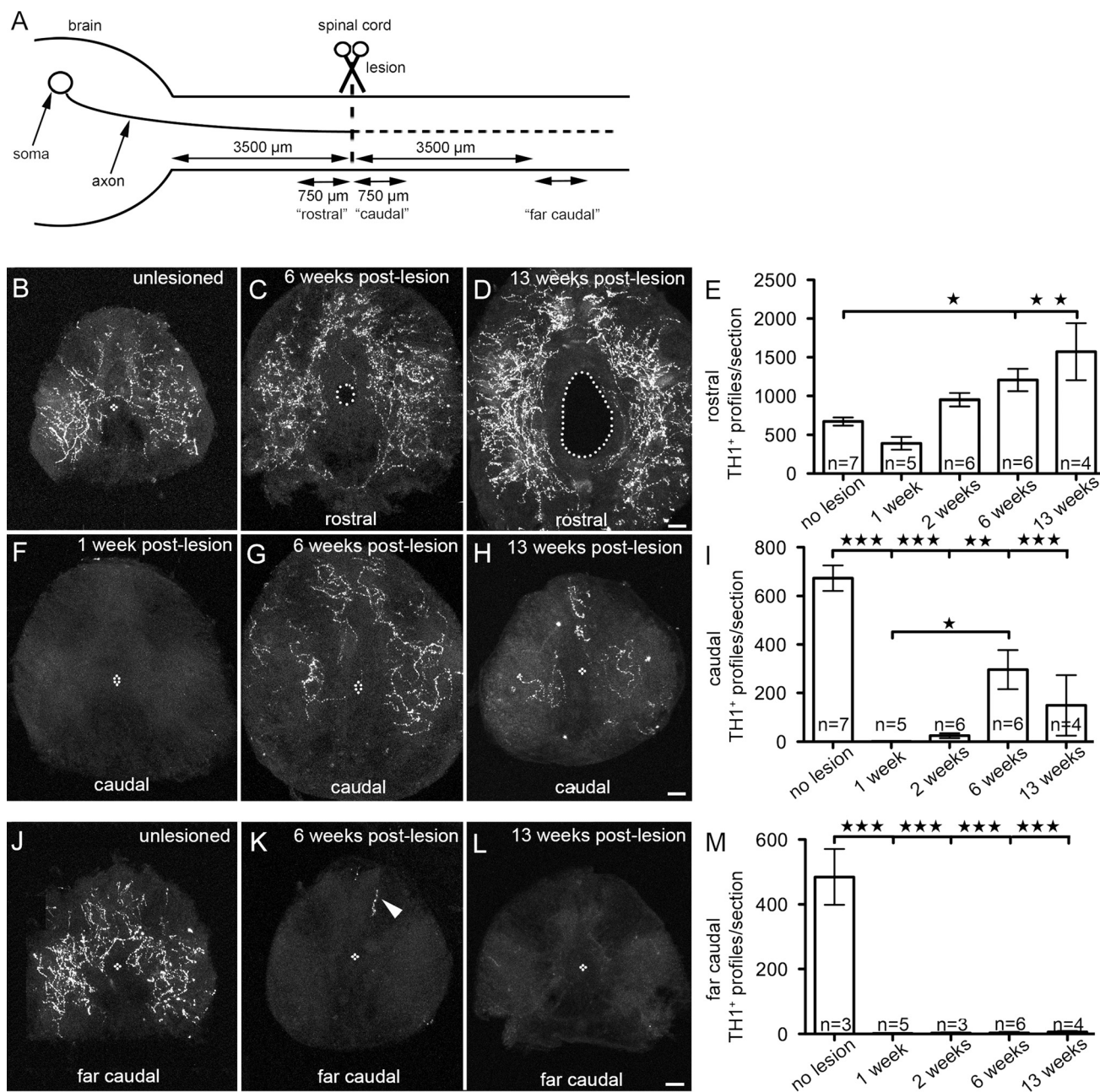


Figure 2. Plasticity of TH1⁺ terminals after spinal lesion. Complete spinal cross sections are shown; dorsal is up, and central canal is outlined by dotted line. **A:** Levels of sectioning. **B:** TH1⁺ terminal varicosities, but no cells are labeled in the unlesioned spinal cord. This section serves as a comparison for C,D,F–H. **C–E:** Numbers of TH1⁺ varicosity profiles increase continuously rostral to the lesion site for at least 13 weeks post lesion. **F–I:** Caudal to the lesion site, all terminals are lost and return of varicosities is observed over time. **J–M:** Re-innervation of a level 3.5 mm caudal to the lesion site is rarely (arrowhead) observed. *, P < 0.05; **, P < 0.01; ***, P < 0.001; Scale bar = 25 μ m in D (applies to B–D), H (applies to F–H), and L (applies to J–L).

held their position in the water flow for 60 minutes. All three animals completely lost their swimming capability (Fig. 3C), and TH1⁺ varicosities were almost completely absent caudal to the lesion site (0.4 ± 0.43 profiles/section, n = 3) 1 week after re-lesion. This indicated that functional recovery was unlikely to be due to plasticity of the spinal circuitry caudal to the lesion site alone and that TH1⁺ re-innervation of the caudal spinal cord after a

lesion was most likely derived from descending axons that regenerated beyond the lesion site.

Lesion-induced quantitative changes in 5-HT terminals in the spinal cord

By using a 5-HT antibody, we detected circuitous axons with numerous varicosities, which were thereby identified

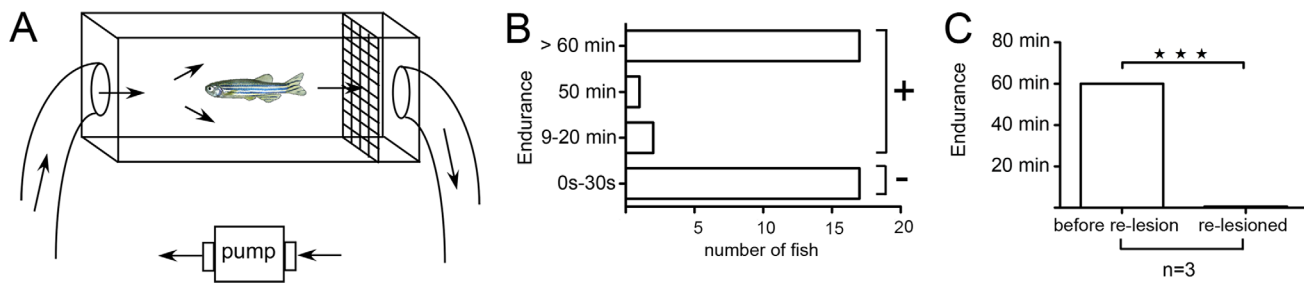


Figure 3. Recovery of swimming capability is variable and is abolished by re-transection of the spinal cord. **A:** A schematic representation of the flow-through tank used to test swim performance. **B:** Fish that were unable to hold their position against a constant water flow for more than 30 seconds were classified as non recovered. **C:** Recovered fish lose their regained swimming ability after re-lesion. [Color figure can be viewed in the online issue, which is available at wileyonlinelibrary.com.]

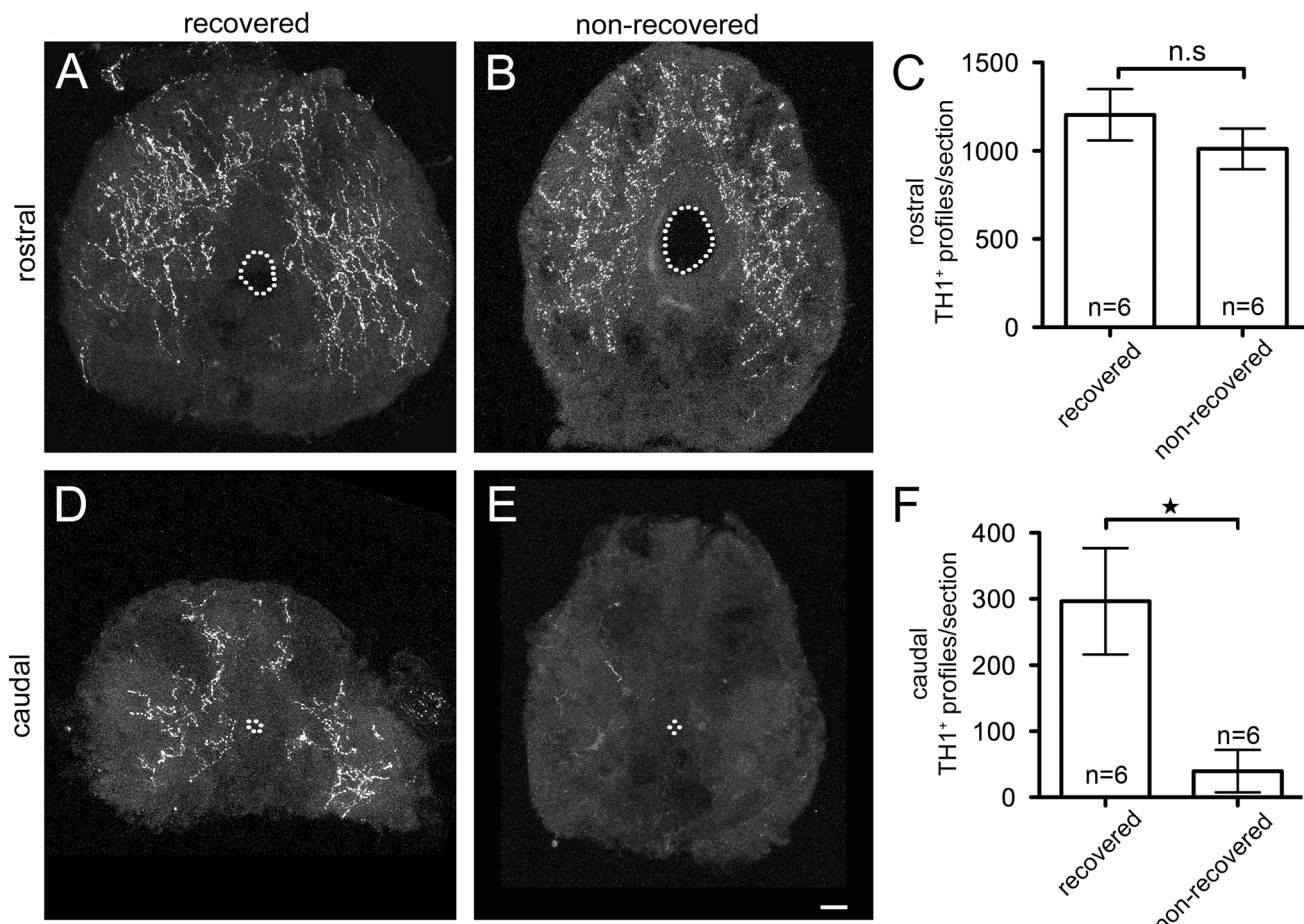


Figure 4. Recovery of swimming capability correlates with re-establishment of TH1⁺ terminals caudal to the lesion site. Complete spinal cross sections are shown; dorsal is up, and central canal is outlined by dotted line. Levels of sectioning are depicted in Figure 2A. **A-C:** Rostral to the lesion site, numbers of TH1⁺ varicosity profiles did not differ between recovered and non recovered fish. **D-F:** Significantly fewer TH1⁺ terminal varicosities from regenerated axons were found caudal to the transection site in non recovered fish than in those showing recovery of swimming capability (*, $P < 0.05$). Scale bar = 25 μ m in E (applies to A,B,D,E).

as axon terminals, in the spinal cord at a midthoracic level (Fig. 5A), and at the level of the dorsal fin (Fig. 6I). Cell bodies were also present in the spinal cord (Fig. 5A). Many of the terminal varicosities were double-labeled

with the synaptic marker SV2 (Fig. 5B-D). By using retrograde tracing from a midthoracic level in combination with 5-HT immunohistochemistry we found double-labeled cells in the inferior raphe region of the brainstem

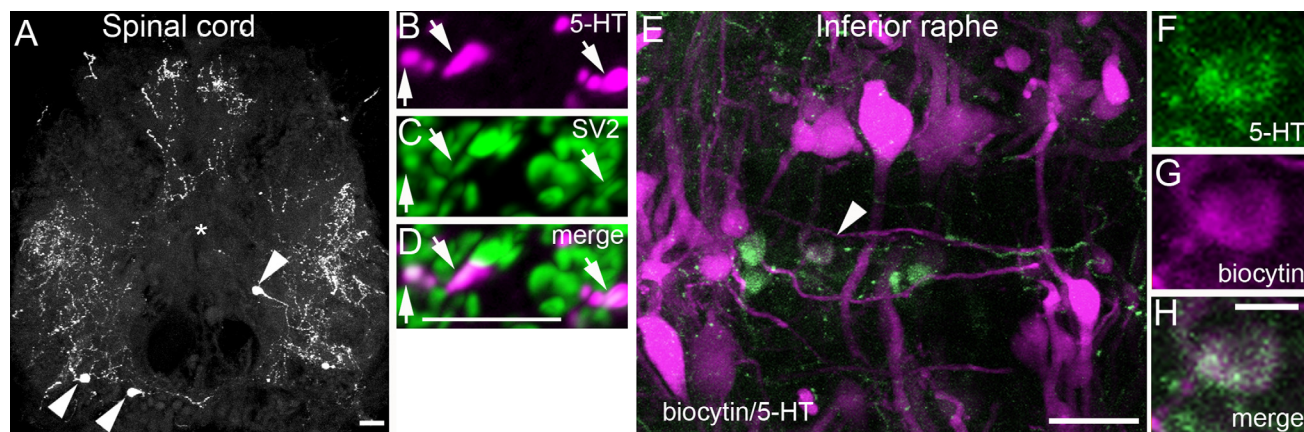


Figure 5. Spinal 5-HT⁺ axons originate in the spinal cord and brainstem. **A:** 5-HT immunohistochemistry on spinal cross sections (dorsal is up) reveals labeled somata (arrowheads) in the ventral spinal cord. The central canal is indicated by an asterisk. **B–D:** 5-HT⁺ terminal varicosities double-label with the synaptic marker SV2 (arrows). **E–H:** A horizontal section through the brainstem is shown; rostral is left. Retrograde tracing from the spinal cord reveals 5-HT immunoreactive somata of neurons in the inferior raphe that project to the spinal cord. A double-labeled cell (arrowhead in **E**) is shown in higher magnification in **F–H**. Scale bar 15 μ m in **A**; 5 μ m in **D** (applies to **B–D**) and **H** (applies to **F–H**); 20 μ m in **E**. [Color figure can be viewed in the online issue, which is available at wileyonlinelibrary.com.]

(Fig. 5E–H), but not in the superior raphe, confirming a previous report of 5-HT⁺ neurons with descending axons in the inferior raphe in adult zebrafish (Lillesaar et al., 2009). Thus 5-HT⁺ terminals in the spinal cord are of supraspinal and local origin.

We established a time course for changes in the density of 5-HT⁺ terminal varicosities after a spinal lesion in the same animals used for TH1 immunohistochemistry, assessing the same locations and time points. In unlesioned animals, 679.1 ± 126.32 profiles/section ($n = 7$) were present. Rostral to the lesion site the number of varicosity profiles was 505.8 ± 36.95 ($n = 5$) at 1 wpl. Thereafter, numbers of varicosity profiles increased until they were 80% higher than in unlesioned animals at 6 wpl (2 wpl: 989.8 ± 155.38 , $n = 6$; 6 wpl: $1,224.1 \pm 105.04$ profiles/section, $n = 6$; $P < 0.05$). At 13 wpl, $1,048.2 \pm 247.04$ profiles/section ($n = 4$) were observed (Fig. 6A–D). This suggested considerable sprouting of 5-HT⁺ axons rostral to the lesion site.

Caudal to the lesion site, the number of varicosity profiles was strongly and significantly reduced at 1 wpl (35.0 ± 5.62 profiles/section, $n = 5$; $P < 0.001$) compared with unlesioned control animals. As opposed to TH1⁺ varicosities, some of the 5-HT⁺ varicosities remained at 1 wpl, suggesting that these originated from local 5-HT⁺ neurons, whereas descending axons and their terminals had undergone Wallerian degeneration at this time point. The numbers of varicosity profiles significantly increased thereafter and peaked at 6 wpl (2 wpl: 103.0 ± 17.41 profiles/section, $n = 6$; 6 wpl: 383.7 ± 71.91 , $n = 6$). The increase in numbers of varicosity profiles between 1 wpl and 6 wpl was statistically significant ($P < 0.05$). At

13 wpl (132.1 ± 19.42 profiles/section, $n = 3$), there was no further increase, compared with 6 wpl (Fig. 6E–H). Thus numbers of varicosity profiles gradually increased again caudal to a lesion site to maximally 58% of the number in unlesioned animals at 6 wpl.

Far caudal to the lesion site, we also observed a huge reduction in numbers of varicosity profiles at 1 wpl (unlesioned: 659.9 ± 110.05 profiles/section, $n = 3$; 1 wpl: 32.5 ± 7.86 , $n = 5$, $P < 0.001$). Numbers of varicosity profiles did not increase until 13 wpl, the latest time point analyzed (2 wpl: 67.8 ± 5.31 profiles/section, $n = 3$; 6 wpl: 91.3 ± 14.23 , $n = 6$; 13 wpl: 64.2 ± 17.85 , $n = 3$; Fig. 6I–L). This suggested that regenerating descending 5-HT⁺ axons did not reach the far caudal level.

The number of 5-HT⁺ varicosity profiles caudal to the lesion site correlates with recovery of swimming capability

Rostral to the lesion site there was no significant difference between recovered ($1,224.1 \pm 105.04$ profiles/section, $n = 6$) and nonrecovered fish (966.8 ± 70.95 profiles/section, $n = 6$, $P > 0.05$) in the number of 5-HT⁺ varicosity profiles at 6 wpl (Fig. 7A–C). In contrast, caudal to the lesion site recovered fish (383.7 ± 71.91 profiles/section, $n = 6$) had significantly more varicosity profiles than nonrecovered ones (88.0 ± 24.12 profiles/section, $n = 6$; $P < 0.01$; Fig. 7D,E,G). This suggested that the quantity of terminal varicosities caudal to the lesion site, derived from re-growth of 5-HT⁺ axons beyond the spinal lesion, was associated with recovery of swimming capability.

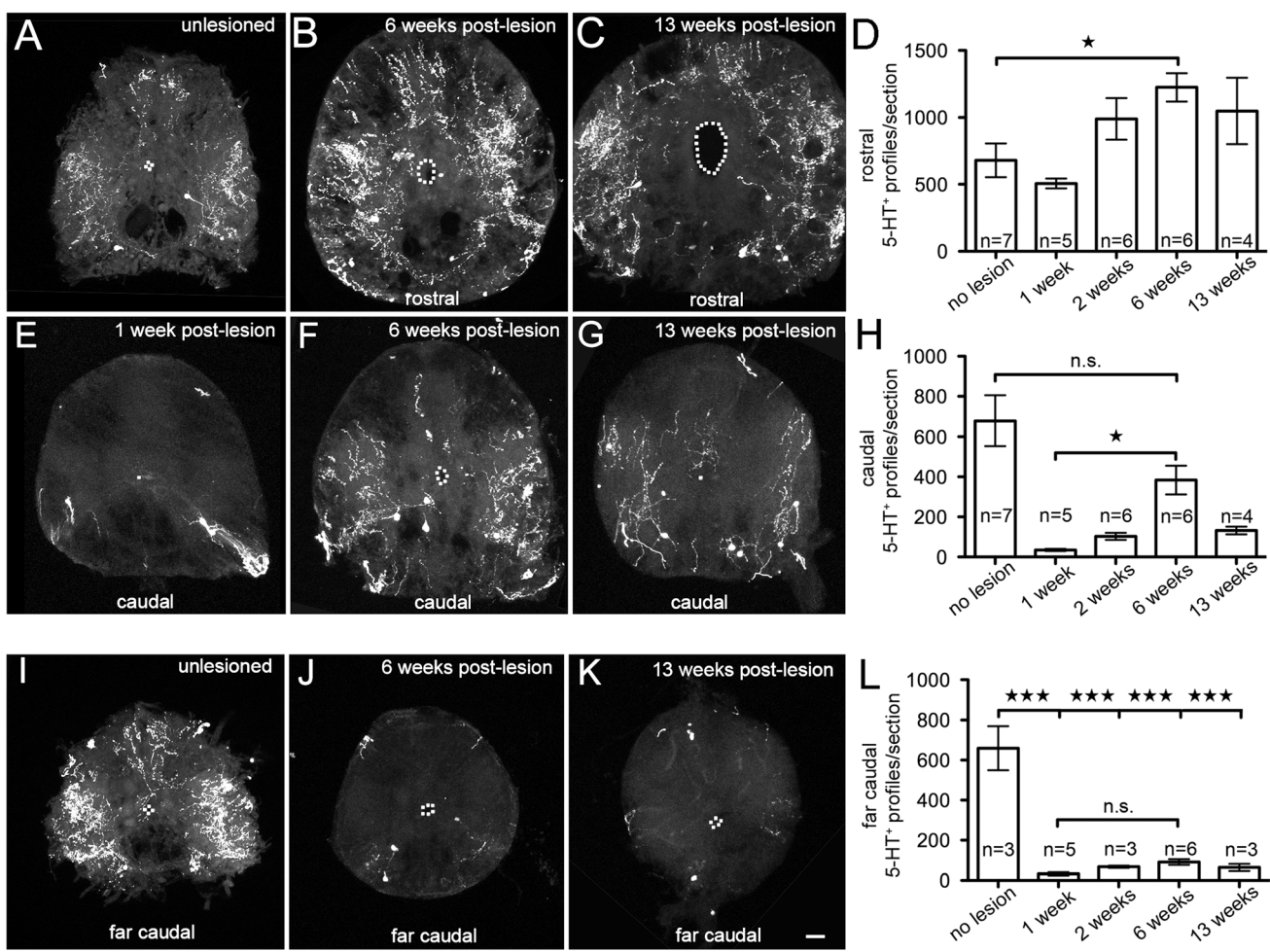


Figure 6. Plasticity of 5-HT⁺ terminals after spinal lesion. Complete spinal cross sections are shown; dorsal is up, and central canal is outlined by dotted line. Levels of sectioning are depicted in Figure 2A. A: 5-HT⁺ terminals and cells are labeled in the unlesioned spinal cord. This section serves as comparison for B, C, E–G. B–D: Numbers of 5-HT⁺ varicosity profiles increase continuously rostral to the lesion site and plateau at 6 weeks post lesion. E–H: Caudal to the lesion site, most varicosities are lost and significant re-innervation is observed at 6 weeks post lesion. I–L: Numbers of varicosity profiles remain low at a level 3.5 mm caudal to the lesion site for at least 13 weeks post lesion. ***, $P < 0.001$; **, $P < 0.01$; *, $P < 0.05$. Scale bar = 25 μ m in K (applies to A–C, E–G, I–K).

The contribution of endogenous spinal neurons to spinal innervation increases after a lesion

By comparing numbers of varicosity profiles at 1 wpl (~ 35 profiles/section) with the unlesioned situation (~ 679 profiles/section), we estimated that local 5-HT cells make a minor contribution ($\sim 5\%$) to spinal 5-HT innervation in unlesioned animals. After re-lesion at 6 wpl and analysis at 1 week after re-lesion, 122.1 ± 32.95 profiles/section ($n = 3$) were observed (Fig. 7F,G). This was a substantial reduction compared with ~ 384 profiles/section observed at 6 wpl, indicating loss of descending axons that had regenerated over the lesion site. Importantly, this also demonstrated a 3.5-fold increase in the number of spinal-derived 5-HT⁺ varicosity profiles after regeneration (1 wpl vs. 1 week after re-lesion: $P < 0.036$). Increased innervation by spinal 5-HT⁺ neurons is probably a consequence of

lesion-induced generation of 5-HT⁺ neurons, as observed in goldfish (Takeda et al., 2008).

Lesion-induced generation of 5-HT⁺ cells

Numbers of 5-HT⁺ cells did not differ significantly between the rostral and caudal level at the different time points and are therefore presented together. Absolute numbers of 5-HT⁺ cells increased steadily after a lesion up to 6 wpl (unlesioned: 93.1 ± 14.17 cells/1,500 μ m spinal cord, $n = 18$; 1 wpl: 120.0 ± 41.13 , $n = 5$; 2 wpl: 363.4 ± 30.41 , $n = 19$; 6 wpl: 471.2 ± 80.57 , $n = 10$; Fig. 8A–C) when the number of 5-HT⁺ cells was 5.1-fold higher than in unlesioned animals ($P < 0.001$). At 13 wpl (217.8 ± 16.70 cells, $n = 5$), a significant reduction in cell number was observed compared with 6 wpl ($P < 0.05$). This number was again comparable to that in unlesioned animals. Far caudal to the lesion site, cell numbers

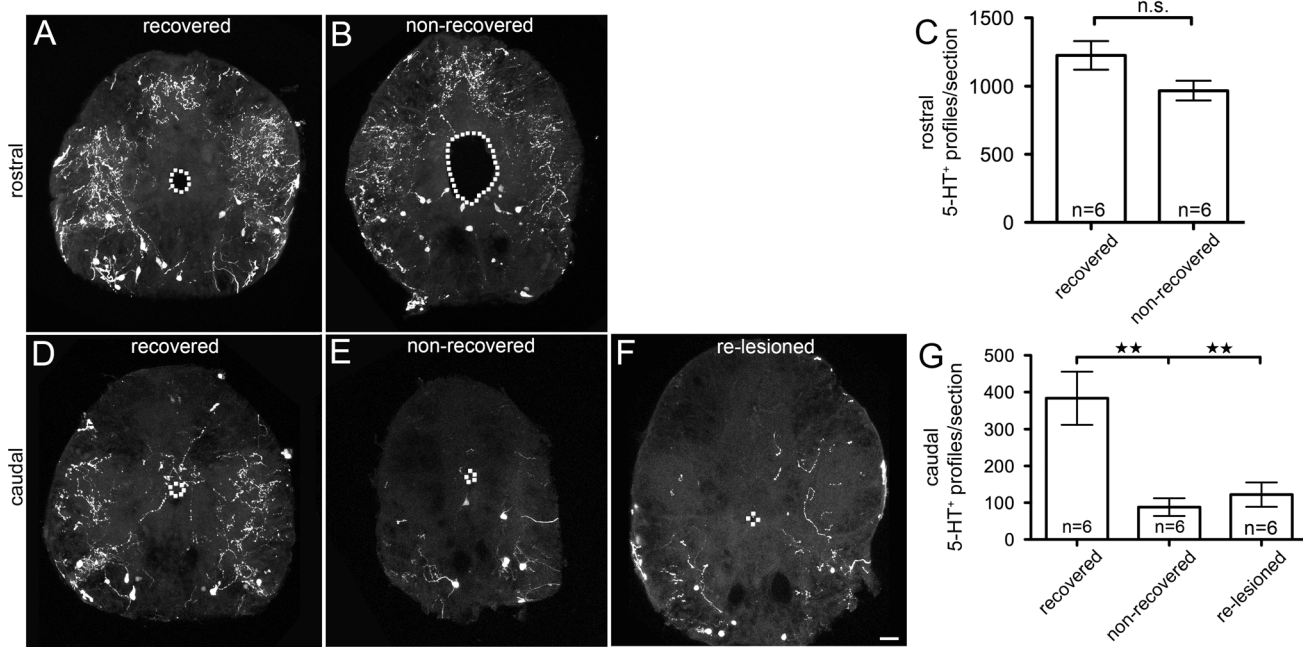


Figure 7. Recovery of swimming capability correlates with re-establishment of 5-HT⁺ terminals caudal to the lesion site. Complete spinal cross sections are shown; dorsal is up, and central canal is outlined by dotted line. Axial levels of sectioning are depicted in Figure 2A. A–C: Rostral to the lesion site, numbers of 5-HT⁺ varicosity profiles do not differ between recovered and non recovered fish. D–G: Significantly fewer 5-HT⁺ varicosity profiles are present caudal to the spinal transection site in non recovered fish (E,G) than in those showing recovery of swimming capability (D). Re-lesion of recovered fish significantly reduces the number of varicosity profiles caudal to the lesion site, indicating that these are mainly derived from descending axons (F,G). **, $P < 0.01$. Scale bar = 25 μm in F (applies to A,B,D–F).

remained unchanged (unlesioned: 200 ± 22.21 cells/ $1,500 \mu\text{m}$, $n = 3$; 1 wpl: 137 ± 30.95 , $n = 5$; 2 wpl: 163.6 ± 29.30 , $n = 3$; 6 wpl: 229.6 ± 35.68 , $n = 6$; 13 wpl: 100.0 ± 34.55), in agreement with previous observations that proliferation in the ventricular progenitor zone is much lower at distant levels (Reimer et al., 2008). Overall, this suggests an overproduction of 5-HT⁺ cells close to the lesion site that is later pruned back.

To directly show that 5-HT⁺ neurons were newly generated after the lesion, we injected animals with the proliferation marker BrdU at 0, 2, and 6 days post lesion. This labeled 74.8 ± 21.10 5-HT⁺/BrdU⁺ cells ($n = 8$) at 2 wpl and 209.8 ± 26.93 cells ($n = 8$) at 6 wpl. No cells were double-labeled in unlesioned fish ($n = 3$; Fig. 8D–I). Even though we presumed that those 5-HT⁺ cells in lesioned animals that exceeded the number in unlesioned fish were newly generated, not all of them were double labeled with BrdU. This was expected, because our BrdU injection scheme also labels only $\sim 25\%$ of newly generated motor neurons after a lesion (Reimer et al., 2008).

We noticed that 5-HT⁺ cells contacted the central canal only in the lesioned spinal cord at 6 and 13 wpl, suggesting that these were recently generated at the central canal. The central canal is lined with the spinal progenitor cells, which are subdivided into dorsoventral expression domains of transcription factors that are simi-

lar to those that give rise to different cell types during embryonic development (Reimer et al., 2008). We found that 5-HT⁺ cells contacting the central canal were not randomly distributed. By double-labeling of 5-HT in olig2:GFP transgenic fish, we found that all 5-HT⁺ cells at the central canal contacted it either ventral to the olig2:GFP⁺ zone ($n = 12$ cells; Fig. 9D–F) or in the olig2:GFP⁺ zone itself ($n = 5$ cells). In shh:GFP transgenic animals, two 5-HT⁺ cells were observed in close proximity to shh:GFP⁺ ependymo-radial glial cells, and five cells appeared to be intermingled with these cells, but were always shh:GFP negative (Fig. 9A–C). However, 5-HT was never co-labeled with olig2:GFP or shh:GFP. This distribution of central canal-contacting 5-HT neurons is consistent with a ventral progenitor zone for 5-HT⁺ neurons after a lesion, comprising the olig2:GFP⁺ zone and a more ventral zone.

Blocking hedgehog activity reduces the number of 5-HT⁺ neurons

The ventral origin of 5-HT neurons after lesion suggests an involvement of hedgehog signaling derived from ventral ependymo-radial glial cells. This has been shown to promote regeneration of motor neurons after a spinal lesion (Reimer et al., 2009). To test this, we used intraperitoneal injections of the Smoothened antagonist cyclopamine,

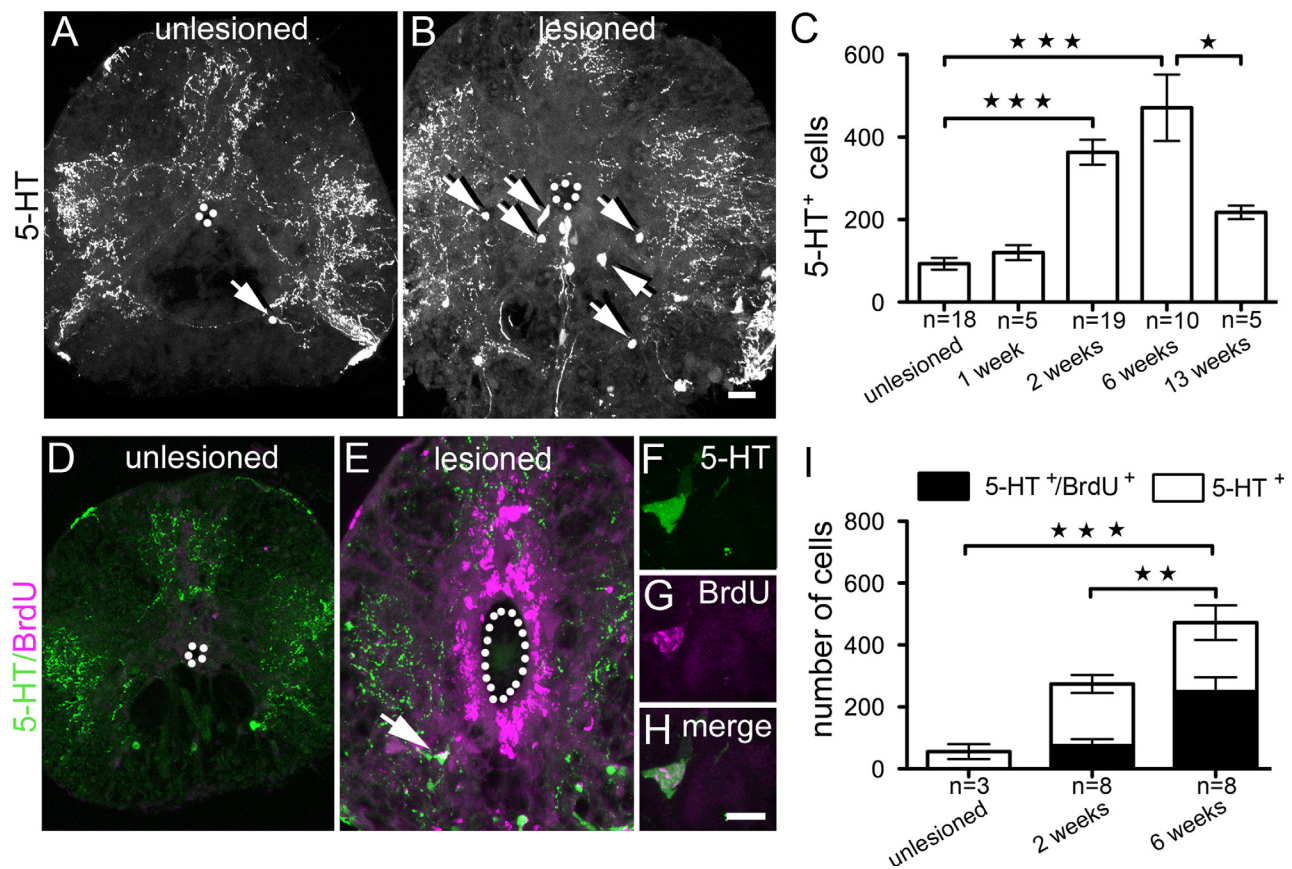


Figure 8. 5-HT⁺ cells are newly generated in the vicinity of a spinal lesion. Complete spinal cross sections are shown; dorsal is up, and central canal is outlined by dotted line. A,B: Arrows depict 5-HT⁺ neurons in the unlesioned (A) and 6 weeks post lesion spinal cord (B). C: Numbers of 5-HT⁺ neurons rise until 6 weeks post lesion and are reduced again at 13 weeks post lesion. D,E: BrdU-labeled 5-HT⁺ cells are detectable at 2 weeks post lesion (E) but not in unlesioned control animals (D). The arrow in E points to a BrdU-labeled 5-HT⁺ cell. F–H: A higher magnification of the double-labeled cell in E is shown. I: A sizable proportion of 5-HT⁺ cells are double labeled with BrdU at different post lesion times. Scale bar = 20 μ m in B (applies to A,B,D,E; 10 μ m in H (applies to F–H). [Color figure can be viewed in the online issue, which is available at wileyonlinelibrary.com.]

previously shown to reduce motor neuron generation and expression of the hedgehog target gene *patched1* in motor neuron progenitor cells (Reimer et al., 2009). Analysis took place at 6 wpl, when the number of newly generated 5-HT⁺ neurons peaked.

Numbers of 5-HT⁺ cells after cyclopamine treatment were significantly reduced by 23% compared with fish injected with the control substance tomatidine (tomatidine: 10.8 ± 0.86 cell profiles/50 μ m, n = 8; cyclopamine: 8.3 ± 1.00 cell profiles/50 μ m; Mann-Whitney U test, one-tailed, $P = 0.0406$). This suggests that shh promotes generation of 5-HT⁺ cells in the lesioned spinal cord.

Numbers of newly generated 5-HT⁺ neurons caudal to the lesion site correlate with recovery of swimming capability and axon re-growth

To determine whether numbers of 5-HT⁺ cells correlate with recovery of swimming capability, we compared num-

bers of 5-HT⁺ cells between recovered and nonrecovered fish at 6 wpl, when cell numbers peak and regenerative success can be assessed. Rostral to the lesion site, differences in 5-HT⁺ cell numbers were not significant between recovered (365.0 ± 73.59 cells/750 μ m, n = 6) and nonrecovered fish (292.6 ± 63.14 cells/750 μ m, n = 6; $P > 0.05$; Fig. 10A–C). In contrast, caudal to the lesion site, fewer 5-HT⁺ cells were present in nonrecovered (111.1 ± 18.59 cells/750 μ m) vs. recovered fish (253.7 ± 28.32 ; $P = 0.0198$; Fig. 10D–F), suggesting some interaction between re-growing axons and newly generated 5-HT⁺ cells.

DISCUSSION

We show for the first time that the TH1 and 5-HT systems are substantially altered in spinal-lesioned zebrafish concomitant with recovery of swimming function (summarized in Fig. 11). Descending axons sprout rostral to the lesion site and regenerate beyond the lesion site for only a short distance, re-establishing about half of the

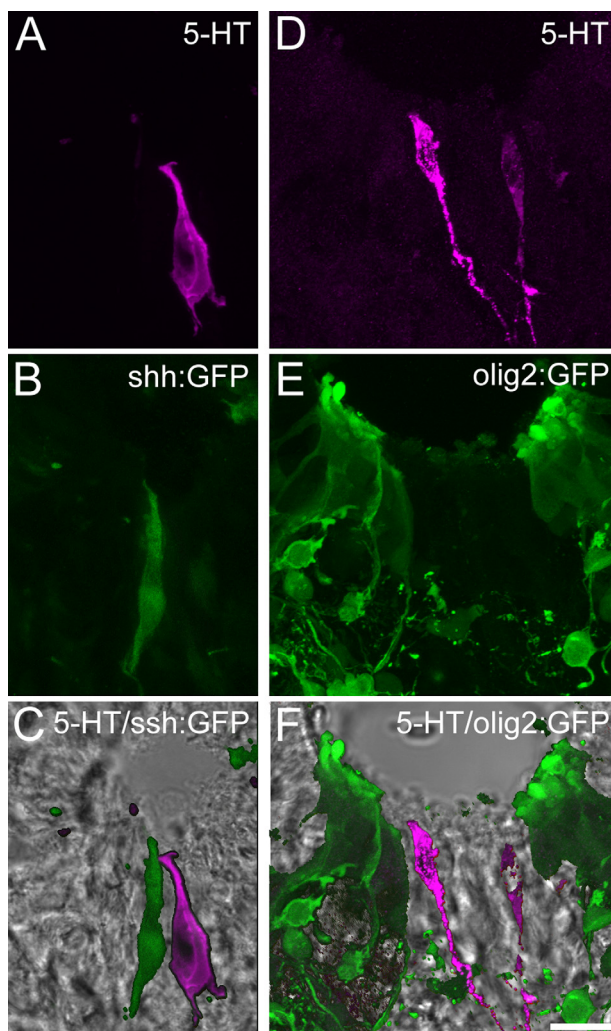


Figure 9. 5-HT^+ cells that contact the central canal in a ventral position are found in the lesioned spinal cord. Cross sections of the ventral ventricular zone at 3 months post lesion are shown; dorsal is up. Ventricular position is depicted in phase-contrast images underlying double labeling in C and F. A–C: Central canal-contacting 5-HT^+ cells are located close to shh:GFP^+ ependymo-radial glial cells. D–F: Central canal-contacting 5-HT^+ cells are located ventral to ventrolateral zones of olig2:GFP^+ ependymo-radial glial cells. Scale bar = 10 μm in F (applies to A–F). [Color figure can be viewed in the online issue, which is available at wileyonlinelibrary.com.]

previous density of terminals. Far caudal positions are not re-innervated. Despite this relatively weak regenerative growth, re-innervation derived from regenerated axons caudal to the lesion site strictly correlates with recovery of function. Spinal-intrinsic 5-HT^+ neurons are first overproduced in the ventral spinal cord in a hedgehog-dependent manner and later pruned back to numbers that are comparable to those in unlesioned animals.

For both TH1^+ and 5-HT^+ descending systems, the abundance of terminals caudal to the lesion site, re-established through axon re-growth beyond the lesion

site, is associated with functional recovery. Importantly, re-lesioning recovered fish abolishes TH1^+ and 5-HT^+ terminals from descending axons caudal to the lesion site, as well as recovered swimming function. This is in agreement with earlier studies showing that fish in which axon re-growth is sparse or experimentally reduced fail to recover (Becker et al., 1997, 2004). Although this suggests that re-innervation of the caudal spinal cord by re-grown TH1^+ and 5-HT^+ axons may be important for recovery of the fish, prelesion patterns are not restored. Both monoaminergic systems studied here re-establish only about half of the terminal varicosities previously observed directly caudal to the lesion site. Moreover, more caudal levels of the spinal cord are mostly not re-innervated.

A previous study also reported re-growth of descending TH1^+ and 5-HT^+ axons in spinal-lesioned zebrafish (van Raamsdonk et al., 1998). However, these limitations were not noticed, due to a lack of quantitative analyses. That study found axon re-growth to 6 mm caudal to the lesion site. We also find terminals derived from long-distance re-growth, which was, however, exceptional, as it was observed in only one of six recovered fish. Even though the functional impact of TH1^+ and 5-HT^+ on spinal function is well documented (see Introduction), TH1^+ and 5-HT^+ axons are only a minority of the axons that do regenerate, and many of these other axons carrying other neuroactive substances reach far caudal levels (Becker et al., 1997), which might have been sufficient to support the observed degree of functional recovery.

What are the reasons for limited re-growth and re-innervation by TH1^+ and 5-HT^+ descending axons? Extrinsic factors, such as a glial scar (Busch and Silver, 2007) or myelin inhibitors (Schwab, 2004) as in mammals are unlikely reasons, because no evidence has been found for either of these in fish (Abdesselem et al., 2009; Becker and Becker, 2002; Nona and Stafford, 1995). Moreover, up to half of the original terminal density is re-established for TH1^+ and 5-HT^+ directly caudal to the transection site, suggesting at least some axon re-growth beyond the lesion site. In addition, many other brain nuclei regenerate axons even into the distal spinal cord (Becker et al., 1997). It is more likely that the axotomy was too distal from the neuronal somata of TH1^+ and 5-HT^+ neurons to elicit a robust regenerative response in descending TH1^+ and 5-HT^+ axons. Indeed, some brain nuclei show a regenerative response, including upregulation of growth-related genes, only when axotomy occurred close to the soma, i.e., after a more rostral spinal lesion (Becker et al., 1998). This is similar to mammalian neurons (Doster et al., 1991; Tetzlaff et al., 1994).

In support of this explanation, we have found robust re-innervation by TH1^+ and 5-HT^+ axons 3.5 mm into the spinal cord in one fish that was lesioned at the brain-stem/spinal cord junction (data not shown). Interestingly,

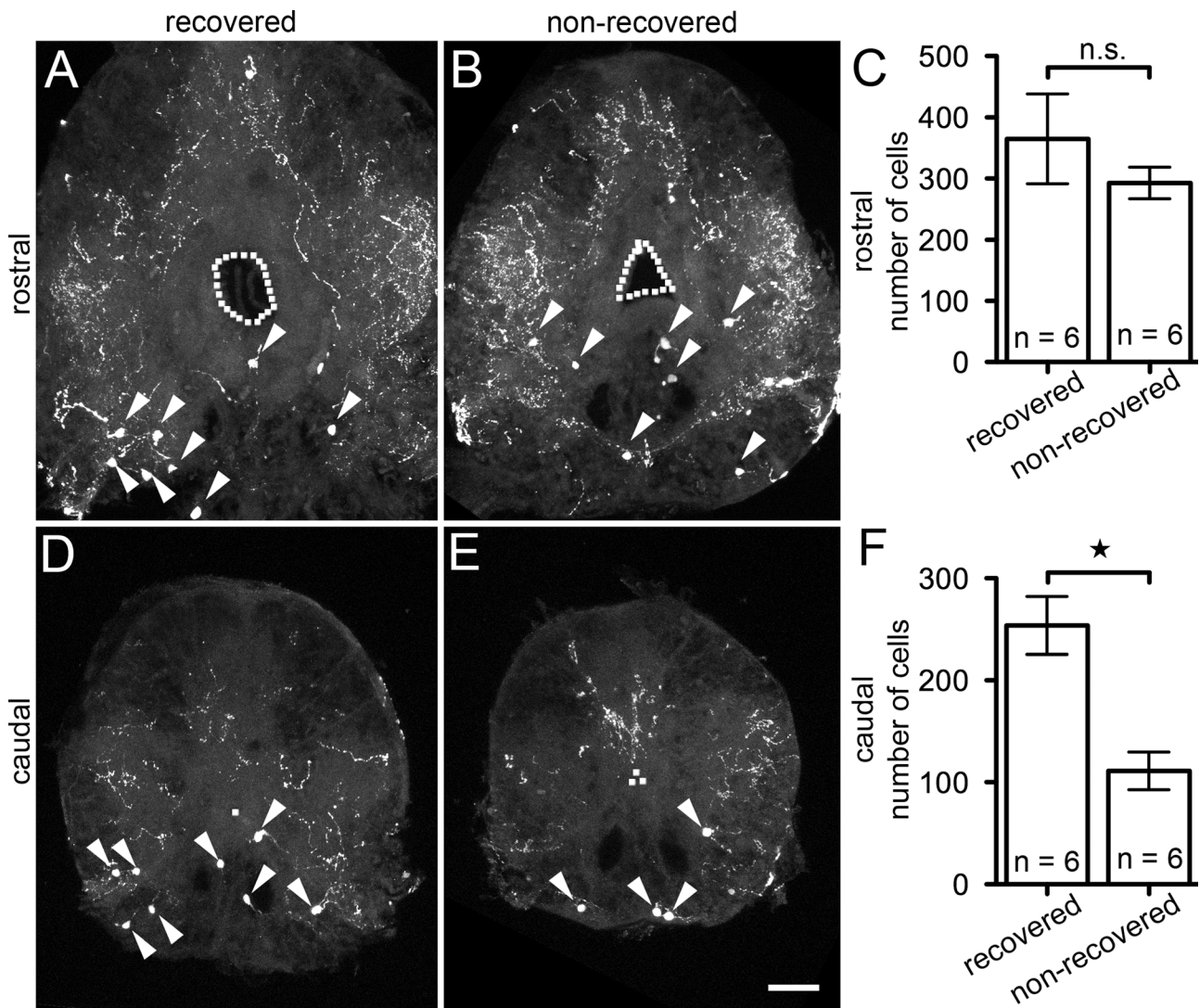


Figure 10. Numbers of 5-HT⁺ cells caudal to the lesion site correlate with recovery of swimming function at 6 weeks post lesion. A,B,D,E: Complete spinal cross sections are shown; dorsal is up, and central canal is outlined by dotted line. Axial levels of sectioning are depicted in Figure 2A. Arrowheads indicate 5-HT⁺ cells. C,F: Cell numbers caudal, but not rostral to the transection site are significantly lower in non recovered fish (*, $P < 0.05$). Scale bar = 50 μ m in E (applies to A,B,D,E).

5-HT⁺ axons have superior sprouting and regenerative capacity compared with other axon types in mammals, demonstrated by their ability to penetrate a glial scar after injury (Hawthorne et al., 2011). Thus, in our lesion model TH1⁺ and 5-HT⁺ cells might not have mounted a significant regenerative response after a lesion at the relatively distal midthoracic level.

Our observations open up the opportunity to learn how successful recovery of function can be achieved with limited anatomical regeneration of specific systems. Apparently, re-innervation of far caudal spinal segments by TH1⁺ and 5-HT⁺ descending axons is not necessary for recovery of substantial swimming function. It is possible that the significantly sprouted TH1⁺ and 5-HT⁺ axons rostral to the lesion site, as well as those axons that did

regenerate into the caudal cord, are capable of modulating the propagating rostrocaudal wave of excitation in the spinal network during swimming (Grillner and Wallen, 2007) without the need to do this at every level of the spinal cord. Alternatively, deficits in function that may be associated with altered TH1⁺ and 5-HT⁺ innervation of the spinal cord might not have been revealed by the functional test of swimming endurance applied here.

Another way in which a lack of long-distance TH1⁺ and 5-HT⁺ descending axons could be compensated for is plasticity of the intraspinal circuitry caudal to the lesion site. For example, spinal intrinsic neurons, which are located at some distance caudal to a lesion site and have not been axotomized by the lesion, upregulate expression of the growth-associated protein 43 and the cell

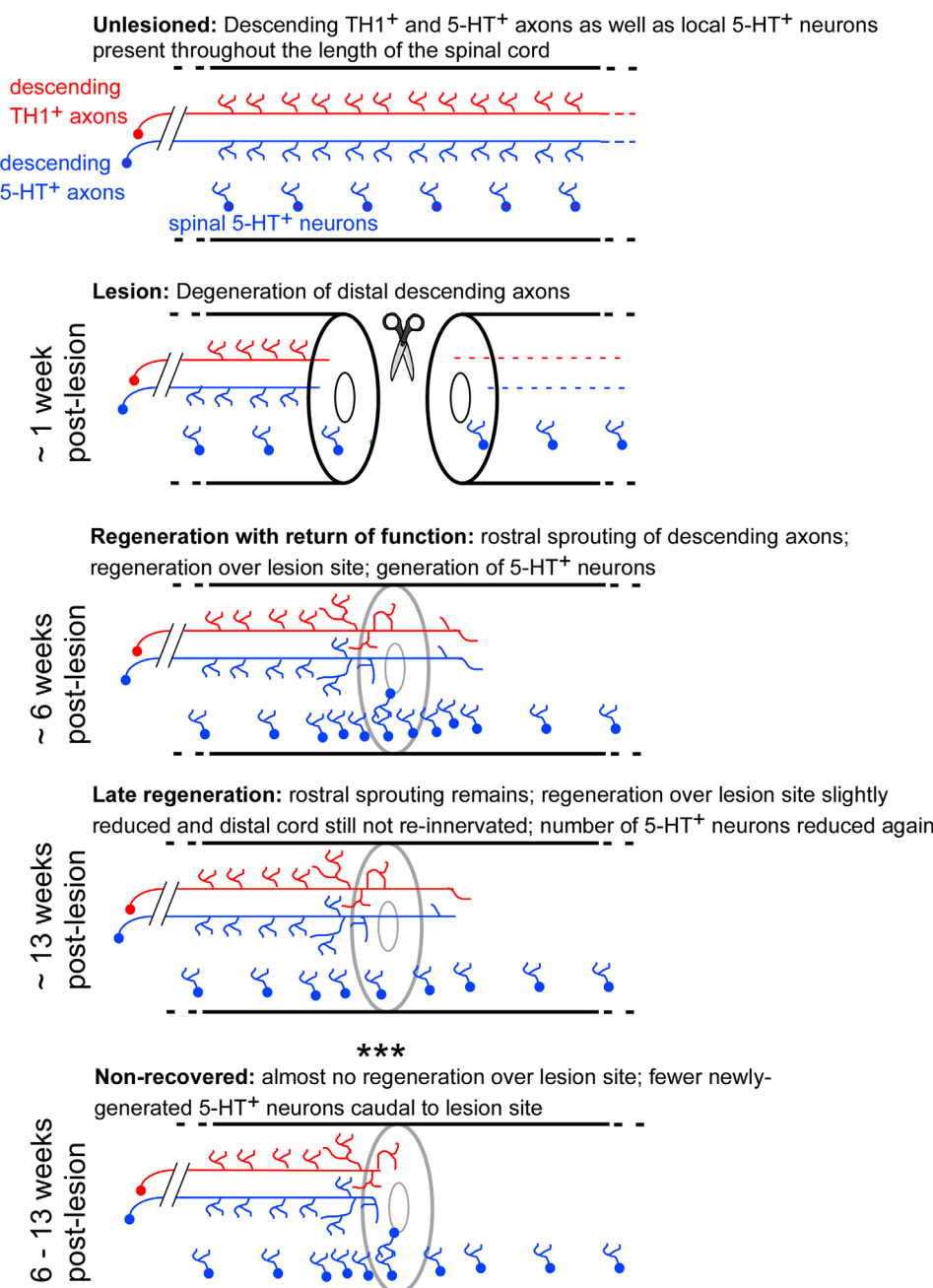


Figure 11. Summary of quantitative changes in TH1⁺ and 5-HT⁺ systems after a spinal lesion. [Color figure can be viewed in the online issue, which is available at wileyonlinelibrary.com.]

recognition molecule L1.1 after a spinal lesion (Becker et al., 2005). Both of these molecules are indicators of neuronal plasticity (Benowitz and Routtenberg, 1997; Emery et al., 2003; Kapfhammer, 1997). Similarly, the rat motor cortex shows plastic changes after ablation of dopaminergic input (Viaro et al., 2011).

Could the loss of innervation by descending 5-HT⁺ axons be offset by newly generated spinal 5-HT⁺ neurons or axonal sprouting of local 5-HT⁺ neurons? Indeed, there is massive generation of 5-HT⁺ cells in the ventral spinal cord, far exceeding the number of cells in unlesioned ani-

mals. However, this increase occurs only in the vicinity of the spinal lesion site, and cell numbers are later pruned back to a level that is no longer significantly elevated over that in unlesioned animals. Sprouting of 5-HT⁺ spinal neurons in the caudal spinal cord that is denervated of descending 5-HT⁺ input could also compensate for a lack of descending input. However, far caudal to the lesion site (not reached by regenerating descending axons), the density of terminal varicosities never significantly increased, despite prolonged (13 weeks) depletion of 5-HT⁺ axons. Thus neither neurogenesis nor axonal

sprouting of spinal-intrinsic 5-HT⁺ cells compensate for lost descending 5-HT⁺ innervation.

Adult zebrafish regenerate spinal 5-HT⁺ neurons in a hedgehog-dependent manner. Our analysis has shown that only during regeneration do radially elongated 5-HT neurons contact the ventricle in adult animals. This is similar to newly generated motor neurons shown to have ventricular contact during spinal cord regeneration (Reimer et al., 2008). Given that lesion-induced proliferation of progenitor cells occurs at the ventricle, this provided us with the opportunity to estimate where 5-HT⁺ cells potentially originate. In contrast to motor neurons, which are born in a narrow olig2:GFP⁺ zone of ependymo-radial progenitor cells, 5-HT⁺ cells appear to have a wider ventral region of origin. Nevertheless, regeneration of this cell type appears to be promoted by a ventral midline-derived hedgehog signal, similar to motor neuron regeneration (Reimer et al., 2009), as determined by blocking this signal with cyclopamine, a strong and specific antagonist of the Hedgehog receptor Smoothened.

Interestingly, in developing mice the descending 5-HT⁺ projection represses the expression of the 5-HT phenotype within a subpopulation of spinal neurons (Branchereau et al., 2002). In our adult regenerating system, descending 5-HT⁺ axons are unlikely to negatively influence neurogenesis of spinal 5-HT⁺ cells, because equal numbers of 5-HT⁺ cells were observed rostral to the lesion site (where descending 5-HT⁺ axons sprouted) and caudal to it (where descending 5-HT⁺ axons were absent) in recovered fish at 2 weeks post lesion. To the contrary, descending axons could even convey a positive signal for spinal neurogenesis, because in animals with few descending axons growing over the lesion site (nonrecovered), also fewer 5-HT⁺ cells were present caudal, but not rostral to the lesion site.

It is important to note that generation of 5-HT⁺ neurons (this report) and motor neurons (Reimer et al., 2008), as well as robust hedgehog signaling, is only detectable in the lesioned spinal cord (Reimer et al., 2009). This is different from neurogenic zones in the brain of zebrafish (Adolf et al., 2006; Kaslin et al., 2009) and mammals (reviewed, for example, in Gould, 2007) that are constitutively active. In the unlesioned spinal cord of zebrafish and mammals, progenitor cells are quiescent (Meletis et al., 2008). However, the lesioned adult spinal cord of zebrafish regenerates different neuronal cell types in a hedgehog-dependent manner, whereas in the mammalian spinal cord only glial cells are generated (Meletis et al., 2008). Therefore, finding the switch that allows proliferation and neurogenesis in the lesioned spinal cord of adult zebrafish is a future goal.

Some changes in the TH1⁺ and 5-HT⁺ systems occurred at late stages of regeneration, between 6 and

13 weeks post lesion, i.e., after functional recovery had been achieved. Most remarkable is the significant reduction in the number of 5-HT⁺ neurons. This could be due to limited trophic support of these cells or to feedback from a rearranged spinal circuitry. Although in the closely related goldfish, a constant increase in the number 5-HT neurons after a spinal lesion was also noted, no reduction was seen at later stages (Takeda et al., 2008). It is possible that this phenomenon only occurs after the last time point analyzed in goldfish. Interestingly, numbers of terminal TH1⁺ and 5-HT⁺ varicosity profiles, derived from descending axons regenerated beyond the lesion site, also appeared to be slightly reduced again at 13 wpl compared with 6 wpl, whereas the sprouted terminals rostral to the lesion site remained. This finding supports the notion that considerable plasticity is occurring in the caudal lesioned spinal cord even after recovery of swimming function.

Overall, our study supports the idea that the lesioned spinal cord of adult zebrafish undergoes substantial axonal and cellular plasticity after a lesion, which leads to functional recovery. Significant alterations in TH1⁺ and 5-HT⁺ systems, including a lack of re-innervation of distal levels of the spinal cord, reveal that for successful spinal cord regeneration, re-establishing the prelesion circuitry is not a prerequisite. However, this and previous studies highlight the importance of axon re-growth over the lesion site for recovery to occur.

ACKNOWLEDGMENTS

We thank Drs. Uwe Strähle and Bruce Appel for transgenic fish, Dr. Wolfgang Driever for plasmids, and Drs. Trudi Gillespie and Roland Wiegand for help with deconvolution software. We are grateful to Maria Rubio for expertly running our zebrafish facility.

LITERATURE CITED

- Abdesselem H, Shypitsyna A, Solis GP, Bodrikov V, Stuermer CA. 2009. No Nogo66- and NgR-mediated inhibition of regenerating axons in the zebrafish optic nerve. *J Neurosci* 29:15489–15498.
- Adolf B, Chapouton P, Lam CS, Topp S, Tannhauser B, Strähle U, Goätz M, Bally-Cuif L. 2006. Conserved and acquired features of adult neurogenesis in the zebrafish telencephalon. *Dev Biol* 295:278–293.
- Becker CG, Becker T. 2002. Repellent guidance of regenerating optic axons by chondroitin sulfate glycosaminoglycans in zebrafish. *J Neurosci* 22:842–853.
- Becker CG, Becker T. 2007. Zebrafish as a model system for successful spinal cord regeneration. In: Becker CG, Becker T, editors. *Model organisms in spinal cord regeneration*. Weinheim: Wiley-VCH. p 289–320.
- Becker CG, Lieberoth BC, Morellini F, Feldner J, Becker T, Schachner M. 2004. L1.1 is involved in spinal cord regeneration in adult zebrafish. *J Neurosci* 24:7837–7842.
- Becker T, Wullimann MF, Becker CG, Bernhardt RR, Schachner M. 1997. Axonal regrowth after spinal cord transection in adult zebrafish. *J Comp Neurol* 377:577–595.

- Becker T, Bernhardt RR, Reinhard E, Wullimann MF, Tongiorgi E, Schachner M. 1998. Readiness of zebrafish brain neurons to regenerate a spinal axon correlates with differential expression of specific cell recognition molecules. *J Neurosci* 18:5789–5803.
- Becker T, Lieberoth BC, Becker CG, Schachner M. 2005. Differences in the regenerative response of neuronal cell populations and indications for plasticity in intraspinal neurons after spinal cord transection in adult zebrafish. *Mol Cell Neurosci* 30:265–278.
- Benowitz LI, Ruttnerberg A. 1997. GAP-43: an intrinsic determinant of neuronal development and plasticity. *Trends Neurosci* 20:84–91.
- Bernstein JJ, Bernstein ME. 1969. Ultrastructure of normal regeneration and loss of regenerative capacity following Teflon blockage in goldfish spinal cord. *Exp Neurol* 24:538–557.
- Boehmler W, Carr T, Thisse C, Thisse B, Canfield VA, Levenson R. 2007. D4 Dopamine receptor genes of zebrafish and effects of the antipsychotic clozapine on larval swimming behaviour. *Genes Brain Behav* 6:155–166.
- Boon KL, Xiao S, McWhorter ML, Donn T, Wolf-Saxon E, Bohnsack MT, Moens CB, Beattie CE. 2009. Zebrafish survival motor neuron mutants exhibit presynaptic neuromuscular junction defects. *Hum Mol Genet* 18:3615–3625.
- Branchereau P, Chapron J, Meyrand P. 2002. Descending 5-hydroxytryptamine raphe inputs repress the expression of serotonergic neurons and slow the maturation of inhibitory systems in mouse embryonic spinal cord. *J Neurosci* 22: 2598–2606.
- Buckley K, Kelly RB. 1985. Identification of a transmembrane glycoprotein specific for secretory vesicles of neural and endocrine cells. *J Cell Biol* 100:1284–1294.
- Busch SA, Silver J. 2007. The role of extracellular matrix in CNS regeneration. *Curr Opin Neurobiol* 17:120–127.
- Chen YC, Priyadarshini M, Panula P. 2009. Complementary developmental expression of the two tyrosine hydroxylase transcripts in zebrafish. *Histochem Cell Biol* 132:375–381.
- Corio M, Peute J, Steinbusch HW. 1991. Distribution of serotonin- and dopamine-immunoreactivity in the brain of the teleost *Clarias gariepinus*. *J Chem Neuroanat* 4:79–95.
- Cornide-Petronio ME, Ruiz MS, Barreiro-Iglesias A, Rodicio MC. 2011. Spontaneous regeneration of the serotonergic descending innervation in the sea lamprey after spinal cord injury. *J Neurotrauma* in press. DOI: 10.1089/neu.2011.1766.
- Doster SK, Lozano AM, Aguayo AJ, Willard MB. 1991. Expression of the growth-associated protein GAP-43 in adult rat retinal ganglion cells following axon injury. *Neuron* 6:635–647.
- Doyle LM, Stafford PP, Roberts BL. 2001. Recovery of locomotion correlated with axonal regeneration after a complete spinal transection in the eel. *Neuroscience* 107:169–179.
- Emery DL, Royo NC, Fischer I, Saatman KE, McIntosh TK. 2003. Plasticity following injury to the adult central nervous system: is recapitulation of a developmental state worth promoting? *J Neurotrauma* 20:1271–1292.
- Filippi A, Mahler J, Schweitzer J, Driever W. 2010. Expression of the paralogous tyrosine hydroxylase encoding genes th1 and th2 reveals the full complement of dopaminergic and noradrenergic neurons in zebrafish larval and juvenile brain. *J Comp Neurol* 518:423–438.
- Gabriel JP, Mahmood R, Kyriakatos A, Soll I, Hauptmann G, Calabrese RL, El Manira A. 2009. Serotonergic modulation of locomotion in zebrafish: endogenous release and synaptic mechanisms. *J Neurosci* 29:10387–10395.
- Gould E. 2007. How widespread is adult neurogenesis in mammals? *Nat Rev Neurosci* 8:481–488.
- Grider MH, Chen Q, Shine HD. 2006. Semi-automated quantification of axonal densities in labeled CNS tissue. *J Neurosci Methods* 155:172–179.
- Grillner S, Jessell TM. 2009. Measured motion: searching for simplicity in spinal locomotor networks. *Curr Opin Neurobiol* 19:572–586.
- Grillner S, Wallen P. 2007. Spinal motor functions in lamprey. In: Becker CG, Becker T, editors. *Model organisms in spinal cord research*. Weinheim: Wiley-VCH. pp 129–144.
- Hawthorne AL, Hu H, Kundu B, Steinmetz MP, Wylie CJ, Deneiris ES, Silver J. 2011. The unusual response of serotonergic neurons after CNS injury: lack of axonal dieback and enhanced sprouting within the inhibitory environment of the glial scar. *J Neurosci* 31:5605–5616.
- Herde MK, Friauf E, Rust MB. 2010. Developmental expression of the actin depolymerizing factor ADF in the mouse inner ear and spiral ganglia. *J Comp Neurol* 518:1724–1741.
- Jing L, Lefebvre JL, Gordon LR, Granato M. 2009. Wnt signals organize synaptic prepattern and axon guidance through the zebrafish unplugged/MuSK receptor. *Neuron* 61: 721–733.
- Jonz MG, Nurse CA. 2003. Neuroepithelial cells and associated innervation of the zebrafish gill: a confocal immunofluorescence study. *J Comp Neurol* 461:1–17.
- Jordan LM, Liu J, Hedlund PB, Akay T, Pearson KG. 2008. Descending command systems for the initiation of locomotion in mammals. *Brain Res Rev* 57:183–191.
- Kapfhamer JP. 1997. Axon sprouting in the spinal cord: growth promoting and growth inhibitory mechanisms. *Anat Embryol (Berl)* 196:417–426.
- Kaslin J, Ganz J, Geffarth M, Grandel H, Hans S, Brand M. 2009. Stem cells in the adult zebrafish cerebellum: initiation and maintenance of a novel stem cell niche. *J Neurosci* 29:6142–6153.
- Kastenhuber E, Kratochwil CF, Ryu S, Schweitzer J, Driever W. 2010. Genetic dissection of dopaminergic and noradrenergic contributions to catecholaminergic tracts in early larval zebrafish. *J Comp Neurol* 518:439–458.
- Kjaerulf O, Kiehn O. 2001. 5-HT modulation of multiple inward rectifiers in motoneurons in intact preparations of the neonatal rat spinal cord. *J Neurophysiol* 85:580–593.
- Leger L, Charnay Y, Hof PR, Bouras C, Cespuglio R. 2001. Anatomical distribution of serotonin-containing neurons and axons in the central nervous system of the cat. *J Comp Neurol* 433:157–182.
- Lieberoth BC, Becker CG, Becker T. 2003. Double labeling of neurons by retrograde axonal tracing and non-radioactive in situ hybridization in the CNS of adult zebrafish. *Methods Cell Sci* 25:65–70.
- Lillesaar C, Stigloher C, Tannhauser B, Wullimann MF, Bally-Cuif L. 2009. Axonal projections originating from raphe serotonergic neurons in the developing and adult zebrafish, *Danio rerio*, using transgenics to visualize raphe-specific pet1 expression. *J Comp Neurol* 512:158–182.
- McClellan AD. 1994. Functional regeneration and restoration of locomotor activity following spinal cord transection in the lamprey. In: Seil FJ, editor. *Progress in Brain Research: Neural Regeneration*. Amsterdam: Elsevier. p 203–217.
- McLean DL, Fetcho JR. 2004. Ontogeny and innervation patterns of dopaminergic, noradrenergic, and serotonergic neurons in larval zebrafish. *J Comp Neurol* 480:38–56.
- McPherson DR, Kemnitz CP. 1994. Modulation of lamprey fictive swimming and motoneuron physiology by dopamine, and its immunocytochemical localization in the spinal cord. *Neurosci Lett* 166:23–26.
- Meletis K, Barnabe-Heider F, Carlen M, Evergren E, Tomilin N, Shupliakov O, Frisen J. 2008. Spinal cord injury reveals multilineage differentiation of ependymal cells. *PLoS Biol* 6:e182.
- Mrini A, Soucy JP, Lafaille F, Lemoine P, Descarries L. 1995. Quantification of the serotonin hyperinnervation in adult

- rat neostriatum after neonatal 6-hydroxydopamine lesion of nigral dopamine neurons. *Brain Res* 669:303–308.
- Neill CM, Meyer MP, Smith SJ. 2004. In vivo imaging of synapse formation on a growing dendritic arbor. *Nat Neurosci* 7:254–260.
- Nona SN, Stafford CA. 1995. Glial repair at the lesion site in regenerating goldfish spinal cord: an immunohistochemical study using species-specific antibodies. *J Neurosci Res* 42: 350–356.
- Olsson C, Holmberg A, Holmgren S. 2008. Development of enteric and vagal innervation of the zebrafish (*Danio rerio*) gut. *J Comp Neurol* 508:756–770.
- Reimer MM, Soärensen I, Kuscha V, Frank RE, Liu C, Becker CG, Becker T. 2008. Motor neuron regeneration in adult zebrafish. *J Neurosci* 28:8510–8516.
- Reimer MM, Kuscha V, Wyatt C, Soärensen I, Frank R, Knüwer M, Becker T, Becker CG. 2009. Sonic hedgehog is a polarized signal for motor neuron regeneration in adult zebrafish. *J Neurosci* 29:15073–15082.
- Schwab ME. 2004. Nogo and axon regeneration. *Curr Opin Neurobiol* 14:118–124.
- Shin J, Park HC, Topczewska JM, Mawdsley DJ, Appel B. 2003. Neural cell fate analysis in zebrafish using olig2 BAC transgenics. *Methods Cell Sci* 25:7–14.
- Shkumatava A, Fischer S, Muller F, Strähle U, Neumann CJ. 2004. Sonic hedgehog, secreted by amacrine cells, acts as a short-range signal to direct differentiation and lamination in the zebrafish retina. *Development* 131:3849–3858.
- Sirbulescu RF, Zupanc GK. 2010. Spinal cord repair in regeneration-competent vertebrates: adult teleost fish as a model system. *Brain Res Rev* 67:73–93.
- Svensson E, Wikstrom MA, Hill RH, Grillner S. 2003. Endogenous and exogenous dopamine presynaptically inhibits glutamatergic reticulospinal transmission via an action of D2 receptors on N-type Ca²⁺ channels. *Eur J Neurosci* 17: 447–454.
- Takeda A, Nakano M, Goris RC, Funakoshi K. 2008. Adult neurogenesis with 5-HT expression in lesioned goldfish spinal cord. *Neuroscience* 151:1132–1141.
- Takeoka A, Kubasak MD, Zhong H, Roy RR, Phelps PE. 2009. Serotonergic innervation of the caudal spinal stump in rats after complete spinal transection: effect of olfactory ensheathing glia. *J Comp Neurol* 515:664–676.
- Tetzlaff W, Kobayashi NR, Giehl KMG, Tsui BJ, Cassar SL, Bedard AM. 1994. Response of rubrospinal and corticospinal neurons to injury and neurotrophins. In: Seil FJ, editor. *Progress in Brain Research: Neural Regeneration*. Amsterdam: Elsevier. p 271–286.
- Thirumalai V, Cline HT. 2008. Endogenous dopamine suppresses initiation of swimming in prefeeding zebrafish larvae. *J Neurophysiol* 100:1635–1648.
- van Raamsdonk W, Bosch TJ, Smitonel MJ, Maslam S. 1996. Organisation of the zebrafish spinal cord: distribution of motoneuron dendrites and 5-HT containing cells. *Eur J Morphol* 34:65–77.
- van Raamsdonk W, Maslam S, de Jong DH, Smit-Onel MJ, Velzing E. 1998. Long term effects of spinal cord transection in zebrafish: swimming performances, and metabolic properties of the neuromuscular system. *Acta Histochem* 100:117–131.
- Viaro R, Morari M, Franchi G. 2011. Progressive motor cortex functional reorganization following 6-hydroxydopamine lesioning in rats. *J Neurosci* 31:4544–4554.
- Westerfield M. 1989. *The zebrafish book: a guide for the laboratory use of zebrafish (*Brachydanio rerio*)*. Eugene, OR: University of Oregon Press.
- Yamamoto K, Ruuskanen JO, Wullimann MF, Vernier P. 2011. Differential expression of dopaminergic cell markers in the adult zebrafish forebrain. *J Comp Neurol* 519:576–598.